René Spencer Chatwell, Jadran Vrabec

Bulk viscosity of liquid noble gases

Chatwell, R. S., & Vrabec, J. (2020). Bulk viscosity of liquid noble gases. The Journal of Chemical Physics, 152(9), 94503. https://doi.org/10.1063/1.5142364

Bulk viscosity of liquid noble gases

René Spencer Chatwell and Jadran Vrabec[a)]

Thermodynamics and Process Engineering, Technische Universität Berlin, 10587 Berlin, Germany

An equation of state for the bulk viscosity of liquid noble gases is proposed. On the basis of dedicated equilibrium molecular dynamics simulations, a multi-mode relaxation ansatz is used to obtain precise bulk viscosity data over a wide range of liquid states. From this data set, the equation of state emerges as a two-parametric power function, with both parameters showing a conspicuous saturation behavior over temperature. After passing a temperature threshold, the bulk viscosity is found to vary significantly over density, a behavior that resembles the frequency response of a one pole low-pass filter. The proposed equation of state is in good agreement with available experimental sound attenuation data.

[a)]Electronic mail: vrabec@tu-berlin.de

I. INTRODUCTION

In contrast to prevailing opinion, bulk viscous effects have widely been explored in fluid mechanics and even share a somewhat controversial history. In 1845 Stokes[1] had argued geometrically that Cauchy's stress tensor field[2]

$$\Pi_{ij} = \Big(\mu_b - \frac{2}{3}\mu_s\Big)\partial_n v_n \delta_{ij} + \mu_s\Big(\partial_j v_i + \partial_i v_j\Big) \ , \tag{1}$$

entails not only the well-known shear viscosity μ_s, but also the bulk viscosity μ_b, which he concurrently postulated to be zero

$$\mu_b \stackrel{!}{=} 0 \ . \tag{2}$$

Stokes, whose proof can hardly be considered rigorous, had limited his argument to incompressible fluids and remained sceptical that his finding (2) would emerge as universally valid. For more than a century, this hypothesis was afflicted with misconceptions until the Royal Society hosted "a discussion on the first and second viscosities of fluids"[3–18] reinvigorating investigations of bulk viscous effects on a wide variety of fluid mechanical problems.

Riemann's solution[19] of the Euler equation[20] was among the first. Retaining the bulk viscosity in the stress tensor field[21] conclusively solved the problem of insensibly small wave thicknesses that were predicted[22,23] in descriptions limited to shear viscosity[24]. The conjectured increase of wave thickness was qualitatively confirmed in successive atomistic simulations of non-ideal liquids[25,26] as well as in numerical investigations of rarefied gases[27–29], given the shock structure is symmetric[30].

Bulk viscous effects have long been considered mere higher-order contributions[31]. However, including the bulk viscosity in the acoustic approximation[32,33] straightforwardly explained the observed second-order fields associated with ultrasonic waves. The vorticity that is generated across a propagating wave's free surface induces a counter-oriented circulatory flow[34–39] that is also known as acoustic streaming or quartz-wind. In hypersonic boundary layer approximations, bulk viscous effects are promoted to second-order in the pressure distribution[40] and even first-order in the outer and inner flow velocities of high Reynolds number flows[41].

In fluids confined to capillaries, the bulk viscosity contributes to first-order in radial pressure and to second-order in the axial velocity[42–47].

Bulk viscous behavior was also investigated for more complex scenarios. An increased

shock wave thickness affects the outer flow's adverse pressure gradient and consequently suppresses the shock induced boundary layer separation[48], while additionally the shock wave's location and strength are much more accurately predicted when bulk viscous effects are included[49]. Likewise, bulk viscous damping has been observed in compressible turbulent flows[50]. A non-zero bulk viscosity enhances kinetic energy dissipation while additionally inhibiting the energy transfer between translational and configurational energy, thus rendering the flow effectively incompressible[51].

Each of the aforementioned investigations, however, has suffered from missing, incomplete or unreliable bulk viscosity data and was consequently restricted to predominantly qualitative results.

II. SOUND ATTENUATION

Since its introduction, the bulk viscosity was closely associated with linear acoustics. Stokes had originally proposed that sound attenuation measurements could confirm his hypothesis (2) experimentally. A propagating wave's linear momentum is dissipated by a surrounding atmosphere, which leads to the exponential decay of its amplitude $A(z)$ over traveled distance $\Delta z = z_2 - z_1$ and is measured by an attenuation coefficient α

$$\frac{A(z_2)}{A(z_1)} = \exp\Big(-\alpha_\lambda \frac{\Delta z}{\lambda}\Big) \ , \tag{3}$$

given here per wavelength λ, i.e. $\alpha_\lambda = \alpha\lambda$. In a first estimate of α_λ for one-dimensional motion, limited to shear viscosity μ_s, Stokes found that the attenuation factorizes into frequency $\omega = 2\pi f$ and a transport function ξ

$$\alpha_\lambda \ = \ \omega \xi^{\text{Stokes}} \ = \ \omega \frac{\pi}{K} \frac{4}{3} \mu_s \ , \tag{4}$$

where $K = \rho c^2$ is the fluid's low-frequency modulus of compression, ρ its density and c its thermodynamic speed of sound. Kirchhoff[52] advanced the discussion by including heat conduction and established that both effects superimpose linearly in the transport function

$$\begin{aligned} \alpha_\lambda^{\text{classical}} &= \omega \Big(\xi^{\text{Stokes}} + \xi^{\text{Kirchhoff}} \Big) \\ &= \omega \frac{\pi}{K} \left(\frac{4}{3} \mu_s + (\kappa - 1) \frac{\gamma}{c_p} \right) \ , \end{aligned} \tag{5}$$

where $\kappa = c_p/c_v$ is the ratio of specific heats and γ the thermal conductivity. The attenuation predicted by this classical theory corresponds ostensibly well with low frequency acoustic measurements.

Subsequently performed ultrasonic measurements[53–57], however, disclosed large deviations from the classical description (5) and motivated Herzfeld[58] and Kneser[59,60] to introduce an additional mechanism

$$\alpha_\lambda = \alpha_\lambda^{\text{classical}} + \alpha_\lambda^{\text{excess}} \ . \tag{6}$$

Both connected classical hydrodynamics to relaxation theory and attributed the excess attenuation $\alpha_\lambda^{\text{excess}}$ to a time lag that occurs during the transfer of energy between the molecules' translational and internal degrees of freedom. In contrast, Tisza[61] refrained from any physical interpretation and incorporated the Herzfeld mechanism into the transport function ξ by force fitting the complex mechanism of relaxation into a scalar valued bulk viscosity[62]

$$\begin{aligned} \alpha_\lambda &= \omega\Big(\xi^{\text{Stokes}} + \xi^{\text{Kirchhoff}} + \xi^{\text{Tisza}}\Big) \\ &= \omega\frac{\pi}{K}\left(\frac{4}{3}\mu_s + (\kappa-1)\frac{\gamma}{c_p} + \mu_b\right) \ . \end{aligned} \tag{7}$$

This extended theory has been validated experimentally up to moderate ultrasonic frequencies, i.e. $f \leq 280$ MHz[63], over a wide range of thermodynamic states.

In the extended vicinity of the critical point, however, an anomalously high attenuation was observed[64–66] that was conclusively attributed to long-range density correlations[67–73], which are alterations of structural relaxation effects[74–77]. The total attenuation partitions into the already established background part (7) and a critical contribution[78,79]

$$\alpha_\lambda^{\text{total}} = \alpha_\lambda + \alpha_\lambda^{\text{critical}} \ . \tag{8}$$

Acoustic dispersion, i.e. the frequency dependent speed of sound $c(\omega)$, confines this critical attenuation to an extended critical region in the thermodynamic state space, cf. supplementary material,

$$\alpha_\lambda^{\text{critical}} = \pi\frac{I(\tilde{\omega})}{J(\tilde{\omega})}\left(\left[\frac{c(\omega)}{c}\right]^2 - 1\right) \ , \tag{9}$$

where $I(\tilde{\omega}), J(\tilde{\omega})$ are improper integrals of a characteristic frequency $\tilde{\omega}$.

III. EXPERIMENTAL DATA

At present, the bulk viscosity is determined experimentally either by non-resonant Rayleigh-Brillouin scattering[80–90] or ultrasonic attenuation measurements[91–121]. Both techniques have successfully been applied to a variety of substances, yet each measurement series was restricted to selective thermodynamic states.

A substantially larger data set, however, can be obtained for liquid noble gases by utilizing their self-similar behavior. While all available sound attenuation measurements for neon, argon, krypton and xenon were evaluated, data subject to critical attenuation were identified and discarded, cf. Fig. 1. The bulk viscosity was calculated on the basis of the ex-

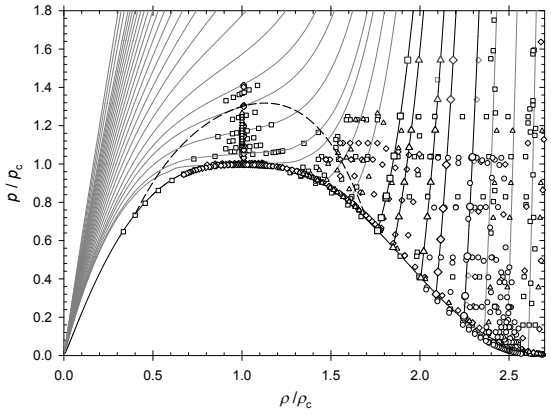

FIG. 1. Overview of thermodynamic states at which experimental sound attenuation data are available for neon[106] (circles), argon[98–101,110,112,113,115,116] (squares), krypton[115–117,119] (triangles) and xenon[79,115,116,118,119,122] (diamonds). *Highlighted*: Seven isotherms were selected $T/T_\mathrm{c} = 0.759$, 0.76, 0.83, 0.86, 0.863, 0.91, 0.93, while $T/T_\mathrm{c} = 0.759$ and 0.863 were omitted in the plot for visibility reasons, along which atomistic simulations were performed to complement and extend the data set to higher pressures $p/p_\mathrm{c} \leq 21$. All thermodynamic states were reduced with the respective fluid's critical pressure p_c and density ρ_c. The extended critical region was constructed on the basis of sound dispersion measurements from the literature and is delimited by the dashed line.

tended classical theory (7) and in contrast to previous works, more accurate thermodynamic data were available by resorting to most recent equations of state[123–127]. Subsequently, μ_b was reduced by a canonical transformation resting on the Lennard-Jones potential, i.e. $\mu_b^\star = \mu_b \sigma^2/\sqrt{m\epsilon}$, with the required set of parameters specified in Tab. I.

Each contribution to bulk viscosity is afflicted by a different uncertainty. While the uncertainty of most recent thermodynamic data are well established to range from $\Delta\rho/\rho = 0.005$ to $\Delta\mu_s/\mu_s = 0.3$ depending on substance and state, the attenuation coefficient α_λ has been determined by single measurements at the respective state point and thus only its absolute maximum errors $\Delta\alpha_\lambda$ has been estimated. Moreover, it is not assured that systematic measurement errors in the literature data, specifically diffraction effects[128], were properly accounted for. Consequently, the reduced bulk viscosity's uncertainty $\Delta\mu_b$ was determined to be linearly affected[129] by its various contributions $\Delta\alpha_\lambda, \Delta c, \Delta\mu_s, \Delta\gamma, \Delta c_v, \Delta c_p$

$$\Delta\mu_b = \left|\frac{K}{\omega\pi}\right| \Delta\alpha_\lambda + ... + \left|\frac{(\kappa-1)\gamma}{c_p^2}\right| \Delta c_p \ . \tag{10}$$

After selecting and evaluating the experimental data, a decline of the bulk viscosity along each isotherm, i.e. from saturation line towards higher densities, can qualitatively be inferred. The effect tends to increase with temperature, however, due to large errors neither the function's gradient nor curvature can accurately be specified, cf. Fig. 2.

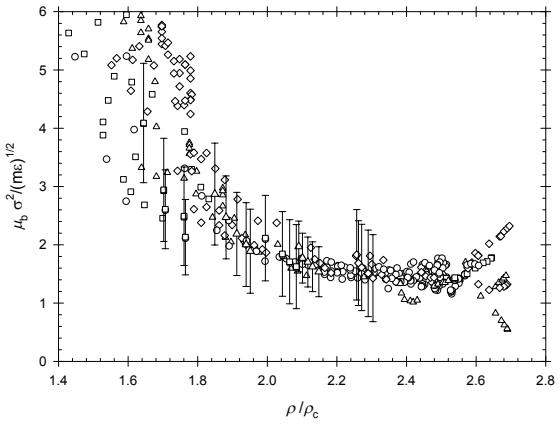

FIG. 2. Overview of bulk viscosity data calculated from the extended classical theory on the basis of experimental sound attenuation data, taken from the literature at the state points indicated in Fig. 1. *Highlighted*: Experimental data at the selected isotherms $T/T_c = 0.76$, 0.83, 0.86, 0.91, 0.96 with their respective uncertainties, calculated from Eq. (10), indicating a monotonic decline of μ_b as a function of density.

TABLE I. The following parameters for the full, i.e. untruncated Lennard-Jones potential σ, ϵ and atomic mass m were used in the canonical transformation[130] to reduce the bulk viscosity and time $t^\star = t\sqrt{\epsilon/(m\sigma^2)}$, where k_B is Boltzmann's constant.

	ϵ/k_B / K	σ / Å	m / u
Ne	33.92	2.801	20.180
Ar	116.79	3.395	39.948
Kr	162.58	3.627	83.798
Xe	226.14	3.949	131.293

IV. MOLECULAR DYNAMICS SIMULATION

To interpret and extend the experimental data set to higher densities, additional bulk viscosity data were sampled by equilibrium molecular dynamics (EMD) simulations along the seven selected isotherms $T/T_\mathrm{c} = 0.759,\ 0.76,\ 0.83,\ 0.86,\ 0.863,\ 0.91,\ 0.93$, cf. Fig. 1. The bulk viscosity was determined microscopically by time-autocorrelation functions of local small-scale, transient pressure fluctuations[131,132] that are intrinsic in any fluid under equilibrium[133]. The Lennard-Jones interaction potential was used, which has demonstrated to resolve such small-scale dynamics adequately and hence successfully describes macroscopic transport in liquid noble gases[134–138].

In the present work, the bulk viscosity's autocorrelation function B_A was sampled in the microcanonical (NVE) ensemble, utilizing the fully open source program $ms2$[139]. The necessary average energies $\langle E \rangle$ were determined by preceding canonical (NVT) ensemble simulations for the given pair of temperature and density. Finite size effects were minimized by placing $N = 4096$ particles in cubic volumes with periodic boundary conditions and choosing a sufficiently large cutoff radius $r_c \geq 5.5\sigma$[140–142]. The employed particle number is well chosen, as simulations containing $N = 12000$ particles yielded virtually identical results, cf. supplementary material. In order to adequately resolve both the existing small-scale dynamics and also the slowly decaying pressure fluctuations[143], a reduced integrator time step $\Delta t^\star = 5 \cdot 10^{-4}$ was specified and each autocorrelation function B_A was sampled over a reduced time period of at least $t^\star \geq 14.6$.

IV.1. Relaxation ansatz

The fluid's intrinsic small-scale pressure fluctuations have conclusively been established to relax in different modes[144–146]. Each mode decays exponentially over time following a Kohlrausch-Williams-Watts function[147,148]. For all of the investigated state points three superimposing relaxation modes were found to be present, leading to the relaxation model's analytical form

$$\begin{aligned} B_R(t) = C_\mathrm{f} \exp\Big(-\Big(\frac{t}{\delta_\mathrm{f}}\Big)^{\beta_\mathrm{f}}\Big) \\ + C_\mathrm{m} \exp\Big(-\Big(\frac{t}{\delta_\mathrm{m}}\Big)^{\beta_\mathrm{m}}\Big) + C_\mathrm{s} \exp\Big(-\Big(\frac{t}{\delta_\mathrm{s}}\Big)^{\beta_\mathrm{s}}\Big) \ . \end{aligned} \tag{11}$$

The first term describes the fast and the subsequent terms the intermediate and slow modes, respectively. The weighting factors are constraint $C_\mathrm{f} + C_\mathrm{m} + C_\mathrm{s} = 1$ and the Kohlrausch parameters δ_i, β_i are a measure of relaxation time scale and distortion from the exponential function, respectively. The eight independent parameters of Eq. (11) were determined by fitting the relaxation model B_R to the sampled autocorrelation function B_A at each state point independently.

Each mode's average relaxation time τ_i is properly defined as integral mean value of its respective contribution $B_{R,i}$ to the relaxation model[149]

$$\tau_i = \frac{1}{C_i} \lim_{t\to\infty} \int_0^t dt\Big(B_{R,i}(t)\Big) \ . \tag{12}$$

As originally proposed by Maxwell, the bulk viscosity μ_b is proportional to the cumulative averaged relaxation time

$$\mu_b = K_r \ \sum_i C_i \tau_i \ , \tag{13}$$

with the proportionality constant K_r being the fluid's relaxation modulus[150].

V. RESULTS

V.1. Relaxation times

The present results are exemplary discussed for states along the isotherm $T/T_\mathrm{c} = 0.86$, yet are qualitatively similar for all other investigated state points as disclosed in the sup-

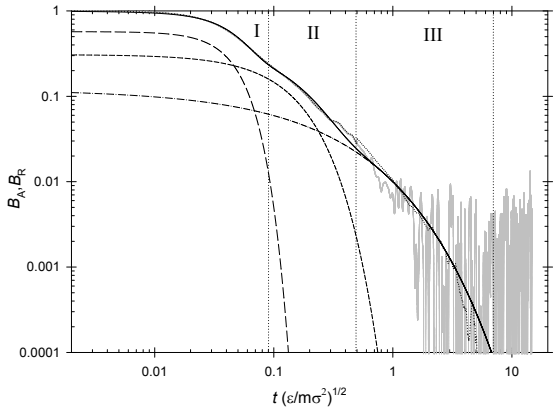

FIG. 3. Comparison of sampled autocorrelation function and relaxation model including all three relaxation modes. The gray line constitutes B_A sampled at $T/T_\mathrm{c} = 0.86$ and $\rho/\rho_\mathrm{c} = 2.06$, while the solid black line represents the relaxation model (11) and its fast, intermediate and slow modes are depicted by dashed, short-dashed and dash-dotted lines, respectively. The post-processed simulation signal (dotted line) is in good agreement with the relaxation model.

plementary material.

The sampled autocorrelation function B_A partitions into three segments, with each segment being dominated by a different mode, cf. Fig. 3. The two dents in the sampled signal readily indicate the fast and intermediate mode's decay. Accompanying the latter, incipiently small scale oscillations are amplified, giving rise to substantial noise contributions in the slow mode. After reconstructing its signal by post-processing, the good agreement between the sampled autocorrelation function B_A and the proposed relaxation model B_R becomes apparent.

More importantly, in contrast to the sampled autocorrelation function that is plagued by noise, the employed relaxation model's time integral properly converges to a definite value, thus allowing to determine the bulk viscosity unambiguously at each state point, cf. Fig. 4.

The average reduced relaxation times τ_i were found to decline exponentially with density for each mode, and to differ roughly by one order of magnitude among the modes up to $\rho/\rho_c \leq 2.2$. While all relaxation modes are increasingly damped with rising density, facilitating shorter relaxation times, the slow mode is damped disproportionately, cf. Fig. 5.

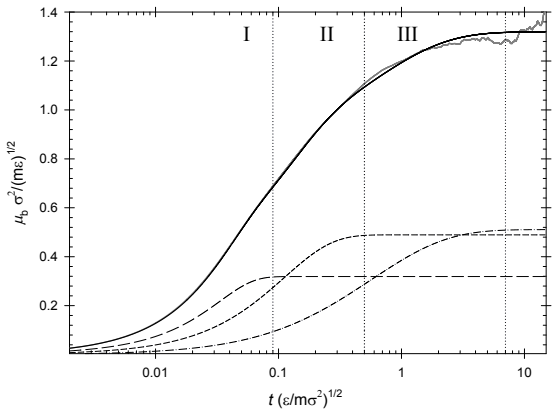

FIG. 4. Comparison of the integrated autocorrelation function B_A with the relaxation model's (11) integral at $T/T_c = 0.86$ and $\rho/\rho_c = 2.06$. Due to noise contributions to B_A, the bulk viscosity μ_b is difficult to determine precisely by molecular dynamics simulation (gray line). In contrast, the proposed relaxation model (solid black line) converges towards an unambiguous value at finite times. The dashed, short-dashed and dot-dashed lines represent the fast, intermediate and slow modes, respectively.

V.2. Equation of state

The most recognized equation of state, of the very few that have actually been discussed in the literature[151,152], relates the bulk viscosity to a power function of density

$$\mu_b \propto \rho^\alpha \ , \tag{14}$$

for which special case solutions with fixed exponents $2\alpha = -1, 0, 1, 3$ exist[153–156]. This proportionality, that was originally proposed in the context of viscous cosmological fluids, is much more universal and also applies to liquid noble gases if the observed temperature dependence is included.

After consolidating all relaxation results, a threshold temperature $T_t/T_c \sim 0.74$ emerges below which the reduced bulk viscosity indicates virtually no variation with density. In contrast, at higher temperatures, μ_b increases progressively towards saturated liquid states, an effect that intensifies with rising temperature, cf. Fig. 6.

While any physically sound equation of state must necessarily establish a unique one-to-one relation between μ_b and each state point, i.e. being bijective, entropy constraints additionally restrict this equation to be non-negative[157,158] and the present results further

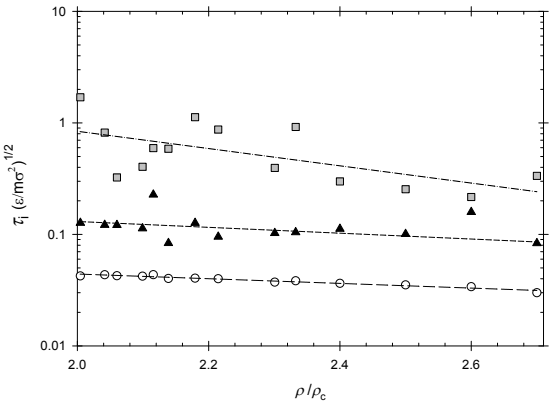

FIG. 5. Distribution of average reduced relaxation times τ_i for all three modes along the isotherm $T/T_c = 0.86$. While each mode is identified to relax exponentially, the slow mode is predominantly affected by increasing density. The symbols represent the relaxation times of the fast τ_s (white circles), the intermediate τ_m (black triangles) and the slow mode τ_s (gray squares), respectively.

specify it to be convex with monotonically decreasing gradient and curvature. Satisfying all conditions, a reduced two-parametric power function is proposed

$$\mu_b^\star = \left(\frac{\rho}{\rho_c} - 1\right)^{\alpha_1} + \alpha_2 \ , \tag{15}$$

with parameters α_1, α_2 depending exclusively on temperature

$$\alpha_i = a_i + b_i \cdot \tanh\left(c_i\left(\frac{T}{T_c} - 1\right)\right) \ . \tag{16}$$

Both parameters, as specified in II, offer a salient saturation behavior that closely resembles the frequency response of a one pole low-pass filter, cf. Fig. 7, causing the fluid to become increasingly more bulk viscous after passing the threshold temperature. This observed temperature dependence is caused by a transition from short-range order, that is present at low temperatures[150], to the long-range density correlations that are intrinsic within the extended critical region. The present equation of state is not only in good agreement with experimental sound attenuation data but also with concurrent MD simulations, cf. Tab. III.

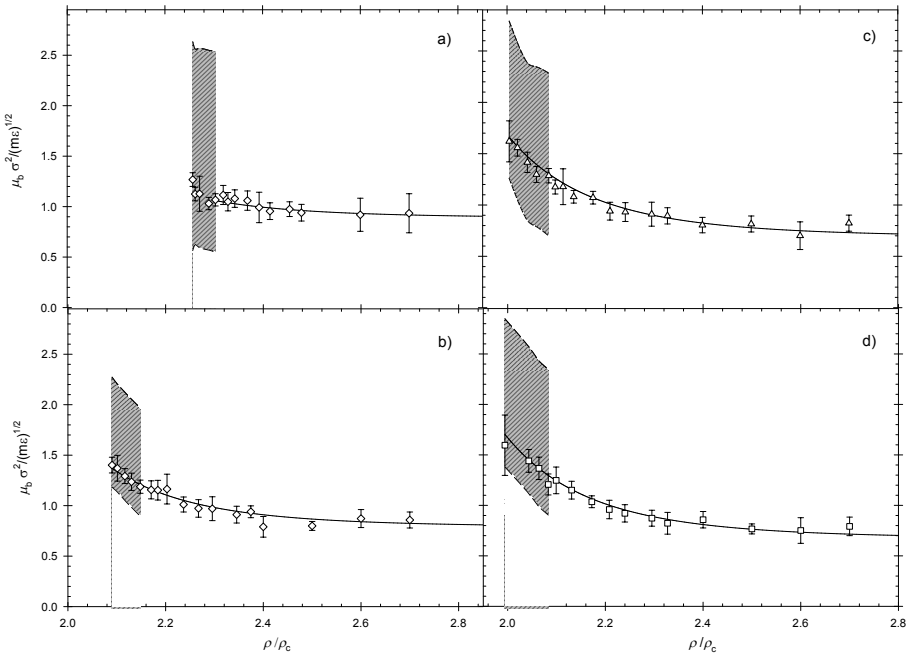

FIG. 6. Outline of bulk viscosity variations from the saturation line towards high density along four isotherms a) $T/T_c = 0.759$, b) $T/T_c = 0.83$, c) $T/T_c = 0.86$ and d) $T/T_c = 0.863$. The grey shaded areas represent the experimentally determined bulk viscosity, according to Eq. (7), including its absolute maximum error, i.e. $\mu_b \pm \Delta\mu_b$, according to Eq. (10). The symbols indicate bulk viscosity data obtained by the employed relaxation ansatz (11) on the basis of the present EMD simulations. The solid line constitute the present equation of state (15).

TABLE II. Best fit parameters a_i, b_i, c_i of Eq. (16).

	a_i	b_i	c_i
α_1	-0.93	5.91	8.67
α_2	-0.53	-1.49	7.86

VI. CONCLUSION

An equation of state for the bulk viscosity of liquid noble gases is proposed. The bulk viscosity originates microscopically from relaxations of small-scale pressure fluctuations, which were found to decay in three different modes, following stretched exponential functions. The slow mode was observed to be disproportionately affected by high density and the average

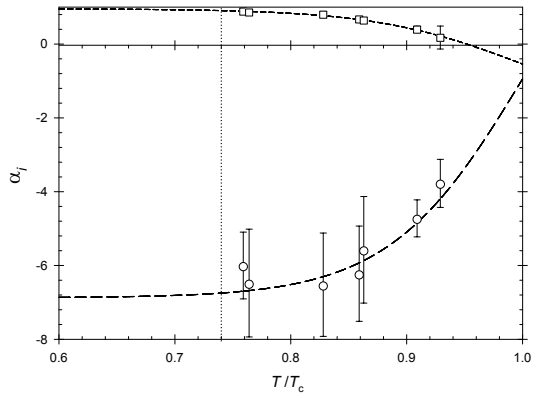

FIG. 7. Variation of parameters α_1 (circles) and α_2 (squares) over temperature. Above the threshold temperature $T/T_c \sim 0.74$ indicated by the vertical line, the bulk viscosity shows a substantial density dependence.

relaxation times τ_i between the modes to differ roughly by one order of magnitude. Each mode was determined on the basis of an autocorrelation function that was straightforwardly sampled by EMD simulations at the respective state point. In order to resolve the slow mode adequately, considerably long autocorrelation functions were necessary.

The equation of state emerges as two-parametric power function with parameters depending exclusively on temperature, cf. Fig. 8. This temperature dependence is attributed to a transition from short-range order that is present at high densities, to long-range density correlations that arise when approaching the extended critical region. After a threshold $T/T_c \sim 0.74$ is passed, the fluid becomes increasingly more bulk viscous. This effect causes sound attenuation to rise progressively with temperature, closely resembling the frequency response of a one pole low-pass filter. In addition, both bulk viscosity coefficients were observed to exhibit opposing behavior, i.e. an increase of bulk viscosity corresponds to a decline of shear viscosity and vice versa, causing the viscosities' ratio to peak $\mu_b/\mu_s \sim 5$ at the highest investigated temperature close to the saturation line.

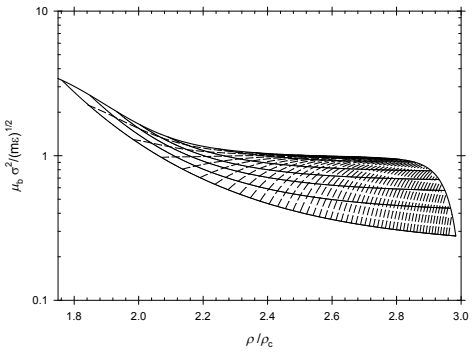

FIG. 8. Illustration of the present equation of state (15). The solid lines constitute the bulk viscosity's variation over density at constant temperature and the dashed lines its variation at constant pressure. The present results straightforwardly explain the experimental results in Fig. (2), which already suggested the bulk viscosity to be a monotonically declining function of density with increasing gradient for higher temperatures.

SUPPLEMENTARY MATERIAL

See the supplementary material for the construction of the critical region, as well as for a full disclosure of all data associated with this manuscript.

ACKNOWLEDGEMENTS

This work was carried out under the auspices of the Boltzmann-Zuse Society (BZS). All simulations were performed either on the HPC clusters OCuLUS and Noctua at the Paderborn Center for Parallel Computing (PC^2) or on the Cray CX40 system *Hazel Hen* at the High Performance Computing Centre Stuttgart (HLRS) with resources allocated according to grant MMHBF2.

REFERENCES

[1]G. G. Stokes, "On the theories of the internal friction of fluids in motion, and of the equilibrium and motion of elastic solids," Cambridge Phil. Soc. **8**, 287 (1845).

[2]A. L. Cauchy, "Recherches sur l'equilibre et le mouvement intérieur des corps solides on fluides, élastiques ou non élastiques," Bull. Soc. Philomath. **2**, 9 (1823).

[3]L. Rosenhead, "Introduction. The second coefficient of viscosity: a brief review of fundamentals," Proc. Royal Soc. A **226**, 1 (1954).

[4]P. E. Doak, "Vorticity generated by sound," Proc. Royal Soc. A **226**, 7 (1954).

[5]E. G. Richardson, "Acoustic experiments relating to the coefficient of viscosity of various liquids," Proc. Royal Soc. A **226**, 16 (1954).

[6]R. O. Davies, "Kinetic and thermodynamic aspects of the second coefficient of viscosity," Proc. Royal Soc. A **226**, 24 (1954).

[7]G. I. Taylor, "The two coefficients of viscosity for an incompressible fluid containing air bubbles," Proc. Royal Soc. A **226**, 34 (1954).

[8]G. I. Taylor, "Note on the volume viscosity of water containing bubbles," Proc. Royal Soc. A **226**, 38 (1954).

[9]R. O. Davies, "A note on Sir Geoffrey Taylor's paper," Proc. Royal Soc. A **226**, 39 (1954).

[10]H. O. Kneser, "Transport and relaxation phenomena," Proc. Royal Soc. A **226**, 40 (1954).

[11]J. E. Piercy and J. Lamb, "Acoustic streaming in liquids," Proc. Royal Soc. A **226**, 43 (1954).

[12]J. H. Andreae and J. Lamb, "Ultrasonic measurements and the second viscosity of carbon disulphide," Proc. Royal Soc. A **226**, 51 (1954).

[13]J. Meixner, "On the thermodynamic theory of the second viscosity," Proc. Royal Soc. A **226**, 51 (1954).

[14]S. M. Karim, "Experimental determination of the second viscosity," Proc. Royal Soc. A **226**, 56 (1954).

[15]J. G. Oldroyd, "Note on the hyrodynamic and thermodynamic pressures," Proc. Royal Soc. A **226**, 57 (1954).

[16]C. A. Truesdell, "The present status of the controversy regarding the bulk viscosity of fluids," Proc. Royal Soc. A **226**, 59 (1954).

[17]E. N. da C. Andrade, "Rewiev of discussion," Proc. Royal Soc. A **226**, 65 (1954).

[18]R. O. Davies and L. Rosenhead, "The two viscosities of fluids," Nature **173**, 1209 (1954).

[19]B. Riemann, "Über die Fortpflanzung ebenener Luftwellen von endlicher Schwingungsbreite," in *Collected works of Bernhard Riemann*, edited by H. Weber (Dover, 1953) p. 157.

[20]L. Euler, "Principes généraux du mouvement des fluides," Mém. Acad. Sci. Berlin **11**, 274 (1755).

[21]D. Gilbarg and D. Paolucci, "The structure of shock waves in the continuum theory of fluids," J. Ration. Mech. Anal. **2**, 617 (1953).

[22]R. Becker, "Stoßwelle und Detonation," Zeitschr. f. Phys. **8**, 321 (1921).

[23]H. Grad, "The profile of a steady shock wave," Comm. Pure and Appl. Math. **5**, 257 (1952).

[24]L. Prandtl, "Zur Theorie des Verdichtungsstoßes," Z. ges. Turbinenwes. **8**, 241 (1906).

[25]W. G. Hoover, "Structure of a shock-wave front in a liquid," Phys. Rev. Lett. **42**, 1531 (1979).

[26]B. L. Holian, W. G. Hoover, B. Moran, and G. K. Straub, "Shock-wave structure via nonequilibrium molecular dynamics and Navier-Stokes continuum mechanics," Phys. Rev. A **22**, 2798 (1980).

[27]G. Emanuel and B. M. Argrow, "Linear dependence of the shock wave thickness on bulk viscosity," Phys. Fluids **6**, 3203 (1994).

[28]T. G. Elizarova, A. A. Khokhlov, and S. Montero, "Numerical simulation of shock wave structure in nitrogen," Phys. Fluids **19**, 068102 (2007).

[29]A. V. Chikitkin, B. V. Rogov, G. A. Tirsky, and S. V. Utyuzhnikov, "Effect of bulk viscosity in supersonic flow past spacecraft," Appl. Numer. Math. **93**, 47 (2015).

[30]S. Taniguchi, T. Arima, T. Ruggeri, and M. Sugiyama, "Overshoot of the non-equilibrium temperature in the shock wave structure of a rarefied polyatomic gas subject to the dynamic pressure," Int. J. Nonlin. Mech. **79**, 66 (2016).

[31]M. van Dyke, "Second-order compressible boundary layer theory with application to blunt bodies in hypersonic flow," in *Hypersonic Flow Research*, edited by F. R. Riddell (Academic Press, 1962) p. 37.

[32]P. M. Morse and K. U. Ingard, *Theoretical Acoustics* (Princeton University Press, 1986).

[33]M. Trusler, *Physical Acoustics and Metrology of Fluids* (CRC Press, 1991).

[34]C. Eckart, "Vortices and streams caused by sound waves," Phys. Rev. **73**, 68 (1948).

[35]L. N. Liebermann, "Second viscosity of liquids," Phys. Rev. **75**, 1415 (1949).

[36]J. J. Markham, "Second-order acoustic fields: Streaming with viscosity and relaxation," Phys. Rev. **86**, 497 (1952).

[37]P. J. Westervelt, "The theory of steady rotational flow generated by a sound field," J. Acoust. Soc. Am. **25**, 60 (1953).

[38]W. L. Nyborg, "Acoustic streaming due to attenuated plane waves," J. Acoust. Soc. Am. **25**, 68 (1953).

[39]J. Lighthill, "Acoustic streaming," J. Sound. Vib. **61**, 391 (1978).

[40]G. Emanuel, "Effect of bulk viscosity on a hypersonic boundary layer," Phys. Fluids **4**, 491 (1992).

[41]M. S. Cramer and F. Bahmani, "Effect of large bulk viscosity on large-Reynolds-number flows," J. Fluid. Mech. **751**, 142 (2014).

[42]H. R. van den Berg, C. A. ten Seldam, and P. S. van der Gulik, "Compressible laminar flow in a capillary," J. Fluid. Mech. **246**, 1 (1993).

[43]J. C. Harley, Y. Huang, H. H. Bau, and J. N. Zemel, "Gas flow in micro-channels," J. Fluid. Mech. **284**, 257 (1995).

[44]Y. Zohar, S. Y. K. Lee, W. Y. Lee, L. Jiang, and P. Tong, "Subsonic gas flow in a straight and uniform microchannel," J. Fluid. Mech. **472**, 125 (2002).

[45]D. C. Venerus, "Laminar capillary flow of compressible viscous fluids," J. Fluid. Mech. **555**, 59 (2006).

[46]E. G. Taliadorou, M. Neophytou, and G. C. Georgiou, "Perturbation solutions of poiseuille flows of weakly compressible Newtonian liquids," J. Non-Newton Fluid. **163**, 25 (2009).

[47]D. C. Venerus and D. J. Bugajsky, "Compressible laminar flow in a channel," Phys. Fluids **22**, 046101 (2010).

[48]F. Bahmani and M. Cramer, "Suppression of large shock-induced separation in fluids having large bulk viscosities," J. Fluid. Mech. **756**, R2 (2014).

[49]S. Bhola and T. K. Sengupta, "Roles of bulk viscosity on transonic shock-wave/boundary layer interactions," Phys. Fluids **31**, 096101 (2019).

[50]S. Chen, X. Wang, J. Wang, M. Wan, H. Li, and S. Chen, "Effects of bulk viscosity on compressible homogeneous turbulence," Phys. Fluids **31**, 085115 (2019).

[51]S. Pan and E. Johnsen, "The role of bulk viscosity on the decay of compressible, homogeneous, isotropic turbulence," J. Fluid. Mech. **833**, 717 (2017).

[52]G. Kirchhoff, "Über den Einfluß der Wärmeleitung in einem Gas auf die Schallbewegung," Ann. Phys. **31**, 691 (1928).

[53]N. Neklepajev, "Über die Absorption kurzer akustischer Wellen in der Luft," Ann. Phys. **340**, 175 (1911).

[54]T. P. Abello, "Absorption of ultrasonic waves by various gases," Phys. Rev. **31**, 1083 (1928).

[55]W. H. Pielemeier, "The Pierce acoustic interferometer as an instrument for the determination of velocity and absorption," Phys. Rev. **34**, 1184 (1929).

[56]E. Großmann, "Schallabsorptionsmessung in Gasen bei hohen Frequenzen," Ann. Phys. **405**, 681 (1932).

[57]R. W. Curtis, "An experimental determination of ultrasonic absorption an reflexion coefficients in air and in carbon dioxide," Phys. Rev. **46**, 811 (1934).

[58]K. F. Herzfeld and F. O. Rice, "Dispersion and absorption of high frequency sound waves," Phys. Rev. **31**, 691 (1928).

[59]H. O. Kneser, "Schallabsorption in mehratomigen Gasen," Ann. Phys. **408**, 337 (1933).

[60]H. O. Kneser, "Schallabsorption und -dispersion in Flüssigkeiten," Ann. Phys. **424**, 277 (1938).

[61]L. Tisza, "Supersonic absorption and Stokes' viscosity relation," Phys. Rev. **61**, 531 (1942).

[62]W. E. Meador, G. A. Miner, and L. W. Townsend, "Bulk viscosity as a relaxation parameter: Fact of fiction?" Phys. Fluids **18**, 258 (1996).

[63]R. A. Rapuano, "Ultrasonic absorption from 75 to 280 Mc/sec," Phys. Rev. **72**, 78 (1947).

[64]W. G. Schneider, "Sound velocity and sound absorption in the critical region," Can. J. Chem. **29**, 243 (1951).

[65]A. G. Chynoweth and W. G. Schneider, "Ultrasonic propagation in xenon in the region of its critical temperature," J. Chem. Phys. **20**, 1777 (1952).

[66]H. D. Parbrook and E. G. Richardson, "Propagation of ultrasonic waves in vapours near the critical point," Proc. Phys. Soc. B **65**, 437 (1952).

[67]M. Fixman, "Ultasonic attenuation in the critical region," J. Chem. Phys. **33**, 1363 (1960).

[68]W. Botch and M. Fixman, "Sound absorption in gases in the critical region," J. Chem. Phys. **42**, 199 (1965).

[69]M. Fixman, "Transport coefficients in the gas critical region," J. Chem. Phys. **47**, 2808 (1967).

[70]K. Kawasaki, "Correlation-function approach to the transport coefficients near the critical point I," Phys. Rev. **150**, 291 (1966).

[71]K. Kawasaki, "Sound attenuation and dispersion near the liquid-gas critical point," Phys. Rev. A **1**, 1750 (1970).

[72]L. P. Kadanoff, W. Götze, D. Hamblen, R. Hecht, E. A. S. Lewis, V. V. Palciauskas, M. Rayl, and J. Swift, "Static phenomena near critical points: Theory and experiment," Rev. Mod. Phys. **39**, 395 (1967).

[73]L. P. Kadanoff and J. Swift, "Transport coefficients near the liquid-gas critical point," Phys. Rev. **166**, 89 (1968).

[74]L. Hall, "The origin of excess ultrasonic absorption in water," Phys. Rev. **71**, 318 (1947).

[75]L. Hall, "The origin of ultrasonic absorption in water," Phys. Rev. **73**, 775 (1948).

[76]D. Sette, "Ultrasonic absorption in liquid mixtures and structural effects," J. Chem. Phys. **21**, 558 (1953).

[77]K. F. Herzfeld and T. A. Litovitz, *Absorption and Dispersion of Ultrasonic Waves* (Academic Press, 1959).

[78]C. W. Garland, D. Eden, and L. Mistura, "Critical sound absorption in xenon," Phys. Rev. Lett. **25**, 1161 (1970).

[79]P. E. Mueller, D. Eden, C. W. Garland, and R. C. Williamson, "Ultrasonic attenuation and dispersion in xenon near its critical point," Phys. Rev. A **6**, 2272 (1972).

[80]P. A. Fleury and J.-P. Boon, "Brillouin scattering in simple liquids: Argon and neon," Phys. Rev. **186**, 244 (1969).

[81]A. S. Pine, "Velocity and attenuation of hypersonic waves in liquid nitrogen," J. Chem. Phys. **51**, 5171 (1969).

[82]B. Y. Baharudin, D. A. Jackson, P. E. Schoen, and J. Rouch, "Bulk viscosity of liquid argon, krypton and xenon," Phys. Lett. A **51**, 409 (1975).

[83]X. Pan, M. N. Shneider, and R. B. Miles, "Coherent Rayleigh-Brillouin scattering," Phys. Rev. Lett. **89**, 183001 (2002).

[84]J. Xu, X. Ren, W. Gong, R. Dai, and D. Liu, "Measurement of the bulk viscosity of liquid by Brillouin scattering," Appl. Opt. **42**, 6704 (2003).

[85]X. Pan, M. N. Shneider, and R. B. Miles, "Power spectrum of coherent Rayleigh-Brillouin scattering in carbon dioxide," Phys. Rev. A **71**, 045801 (2005).

[86]A. S. Meijer, A. S. de Wijn, M. F. E. Peters, N. J. Dam, and W. van de Water, "Coherent Rayleigh-Brillouin scattering measurements of bulk viscosity of polar and nonpolar gases, and kinetic theory," J. Chem. Phys. **133**, 164315 (2010).

[87]X. He, H. Wei, J. Shi, J. Liu, S. Li, W. Chen, and X. Mo, "Experimental measurement of bulk viscosity of water based on stimulated Brillouin scattering," Opt. Commun. **285**, 4120 (2012).

[88]Z. Gu and W. Ubachs, "A systematic study of Rayleigh-Brillouin scattering in air, N_2 and O_2 gases," J. Chem. Phys. **141**, 104320 (2014).

[89]Z. Gu, W. Ubachs, and W. van de Water, "Rayleigh-Brillouin scattering of carbon dioxid," Opt. Lett. **39**, 3301 (2014).

[90]Y. Ma, H. Li, Z. Gu, W. Ubachs, Y. Yu, J. Huang, B. Zhou, Y. Wand, and K. Liang, "Analysis of Rayleigh-Brillouin spectral profiles and Brillouin shifts in nitrogen gas and air," Opt. Express **22**, 2092 (2014).

[91]G. W. Pierce, "Piezoelectric crystal oscillators applied to the precision measurement of the velocity of sound in air and CO_2 at high frequency," Proc. Am. Acad. Arts Sci. **60**, 271 (1925).

[92]M. Kohler, "Schallabsorption in Mischungen einatomiger Gase," Ann. Phys. **431**, 209 (1941).

[93]J. M. M. Pinkerton, "The absorption of ultrasonic waves in liquids and its relation to molecular constitution," Proc. Royal Soc. B **62**, 129 (1949).

[94]M. Pancholy, "Temperature variation of velocity and absorption coefficient of ultrasonic waves in heavy water," J. Acoust. Soc. Am. **25**, 1003 (1953).

[95]T. A. Litovitz and E. H. Carnevale, "Effect of pressure on sound propagation in water," J. Appl. Phys. **26**, 816 (1955).

[96]W. Tempest and H. D. Parbrook, "The absorption of sound in argon, nitrogen and oxygen," Acustica **7**, 354 (1957).

[97]D. G. Naugle and C. F. Squire, "Ultrasonic attenuation in liquid argon," J. Chem. Phys. **42**, 3725 (1965).

[98]D. G. Naugle, "Excess ultrasonic attenuation and intrinsic volume viscosity in liquid argon," J. Chem. Phys. **44**, 741 (1966).

[99]D. G. Naugle, J. H. Lunsford, and J. R. Singer, "Volume vicosity in liquid argon at high pressure," J. Chem. Phys. **45**, 4669 (1966).

[100]D. S. Swyt, J. F. Havlice, and E. F. Carome, "Ultrasonic absorption in liquid argon," J. Chem. Phys. **47**, 1199 (1967).

[101]W. M. Madigosky, "Density dependence of bulk viscosity in argon," J. Chem. Phys. **46**, 4441 (1967).

[102]J. R. Singer and J. H. Lunsford, "Ultrasonic attenuation and volume viscosity in liquid nitrogen," J. Chem. Phys. **47**, 811 (1967).

[103]J. R. Singer, "Excess ultrasonic attenuation and volume viscosity in liquid methane," J. Chem. Phys. **51**, 4729 (1969).

[104]A. E. Victor and R. T. Beyer, "Ultrasonic absorption in liquid oxygen and nitrogen," J. Chem. Phys. **52**, 1573 (1970).

[105]J. Allegra, S. Hawley, and G. Holton, "Pressure dependence of the ultrasonic absorption in toluene and hexane," J. Acoust. Soc. Am. **47**, 144 (1970).

[106]E. V. Larson, D. G. Naugle, and T. W. Aldair, "Ultrasonic velocity and attenuation in liquid neon," J. Chem. Phys. **54**, 2429 (1971).

[107]S. K. Kor, O. N. Awasthi, G. Rai, and S. C. Deorani, "Structural absorption of ultrasonic waves in methanol," Phys. Rev. A **3**, 390 (1971).

[108]S. K. Kor, S. C. Deorani, and B. K. Singh, "Origin of ultrasonic absorption in methanol," Phys. Rev. A **3**, 1780 (1971).

[109]S. K. Kor, S. C. Deorani, B. K. Singh, R. Prasad, and U. Tandon, "Ultrasonic study of structural relaxation in ethanol," Phys. Rev. A **4**, 1299 (1971).

[110]J. A. Cowan and R. N. Ball, "Temperature dependence of bulk viscosity in liquid argon," Can. J. Phys. **50**, 1881 (1972).

[111]G. Rai, B. K. Singh, and O. N. Awasthi, "Structural absorption of ultrasonic waves in associated liquids," Phys. Rev. A **5**, 918 (1972).

[112]J. A. Cowan and P. W. Ward, "Ultrasonic attenuation of the bulk viscosity of liquid argon near the critical point," Can. J. Phys. **51**, 2219 (1973).

[113]P. W. Ward, J. A. Cowan, and R. K. Pathria, "Critical attenuation of ultrasound in argon," Can. J. Phys. **53**, 29 (1975).

[114]G. J. Prangsma, A. J. Alberga, and J. J. M. Beenakker, "Ultrasonic determination of the volume viscosity of N_2, CO and CD_4 between 77 and 300 K," Physica **64**, 278 (1973).

[115]S. A. Mikhailenko, B. G. Dudar, and V. A. Shmidt, "Volume viscosity and relaxation times in monoatomic classical fluids," Fiz. Nizk. Temp. **1**, 224 (1975).

[116]P. Malbrunot, A. Boyer, E. Charles, and H. Abachi, "Experimental bulk viscosities of argon, krypton and xenon near their triple point," Phys. Rev. A **27**, 1523 (1983).

[117]J. A. Cowan and R. N. Ball, "Ultrasonic attenuation and bulk viscosity in liquid krypton," Can. J. Phys. **58**, 74 (1980).

[118]J. A. Cowan and J. W. Leech, "Ultrasonic attenuation and bulk viscosity of liquid xenon," Can. J. Phys. **59**, 1280 (1981).

[119]J. A. Cowan and J. W. Leech, "Critical region ultrasonic attenuation in the condensed inert gases," Can. J. Phys. **61**, 895 (1983).

[120]A. S. Dukhin and P. J. Goetz, "Bulk viscosity and compressibility measurement using acoustic spectroscopy," J. Chem. Phys. **120**, 124519 (2009).

[121]M. J. Holmes, N. G. Paker, and M. J. W. Povey, "Temperature dependence of bulk viscosity in water using acoustic spectroscopy," J. Phys. Conf. Ser. **269**, 012011 (2011).

[122]J. Thoen and C. W. Garland, "Sound absorption and dispersion as a function of density near the critical point of xenon," Phys. Rev. A **10**, 1311 (1974).

[123]C. Tegeler, R. Span, and W. Wagner, "A new equation of state for argon covering the fluid region for temperatures from the melting line to 700 K at pressures up to 1000 MPa," J. Phys. Chem. Ref. Data **28**, 779 (1999).

[124]E. W. Lemmon and R. T. Jacobsen, "Viscosity and thermal conductivity equations for nitrogen, oxygen, argon and air," In. J. Thermophys. **25**, 21 (2004).

[125]E. W. Lemmon and R. Span, "Short fundamental equations of state for 20 industrial fluids," J. Chem. Eng. Data **51**, 785 (2006).

[126]M. L. Huber, "Models for viscosity, thermal conductivity, and surface tension of selected pure fluids as implemented in refprop v10.0," Tech. Rep. (National Institute for Standards and Technology, 2014).

[127]R. Katti, R. T. Jacobsen, R. B. Stewart, and M. Jahangiri, "Thermodynamic Properties of Neon for Temperatures from the Triple Point to 700 K at Pressures to 700 MPa," in *Advances in Cryogenic Engineering*, edited by R. W. Fast (Springer, 1986) pp. 1189–1197.

[128]L. Claes, L. M. Hülskämper, E. Baumhögger, N. Feldmann, R. S. Chatwell, J. Vrabec, and B. Henning, "Acoustic absoprtion measurement for the determination of the bulk viscosity of pure fluids," TM - Tech. Mess. **86**, 2–6 (2019).

[129]J. R. Taylor, *Introduction to Error Analysis: the Study of Uncertainties in Physical Measurements*, 2nd ed. (University Science Books, 1997).

[130]G. Rutkai, M. Thol, R. Span, and J. Vrabec, "How well does the Lennard-Jones potential represent the thermodynamic properties of noble gases?" Mol. Phys. **115**, 1104 (2017).

[131]M. S. Green, "Markoff random process and the statistical mechanics of time-dependent phenomena. II. Irreversible processes in fluids," J. Chem. Phys. **22**, 398 (1954).

[132]R. Kubo, "Statistical-mechanical theory of irreversible processes. I. General theory of simple applications to magnetic and conductive problems," J. Phys. Soc. Jpn. **12**, 570 (1957).

[133]R. Kubo, "The fluctuation-dissipation theorem," Rep. Prog. Phys. **29**, 255 (1966).

[134]L. Verlet, "Computer "experiments" on classical fluids. (I). Properties of Lennard-Jones molecules," Phys. Rev. **159**, 98 (1967).

[135]D. Levesque and L. Verlet, "Computer "experiments" on classical fluids. (III). Time-dependent self-correlation functions," Phys. Rev. A. **2**, 2514 (1970).

[136]D. Levesque, L. Verlet, and J. Kürkijarvi, "Computer "experiments" on classical fluids. (IV). Transport properties and time-correlation functions of the Lennard-Jones liquid near its triple point," Phys. Rev. A. **7**, 1690 (1973).

[137]S. V. Lishchuk, "Role of three-body interactions in formation of bulk viscosity in liquid argon," J. Chem. Phys. **136**, 164501 (2012).

[138]F. Jaeger, O. K. Matar, and E. A. Müller, "Bulk viscosity of molecular liquids," J. Chem. Phys. **148**, 174504 (2018).

[139]G. Rutkai, A. Köster, G. Guevara-Carrion, T. Janzen, M. Schappals, C. W. Glass, M. Bernreuther, A. Wafai, S. Stephan, M. Kohns, S. Reiser, S. Deublein, M. T. Horsch, H. Hasse, and J. Vrabec, "ms2: A molecular simulation tool for thermodynamic properties, release 3.0," Comput. Phys. Commun. **221**, 343 (2017).

[140]K. Meier, A. Laesecke, and S. Kabelac, "Transport coefficients of the Lennard-Jones model fluid. III. Bulk viscosity," J. Chem. Phys. **122**, 014513 (2005).

[141]V. G. Baidakov and S. P. Protsenko, "Metastable Lennard-Jones fluids. III. Bulk viscosity," J. Chem. Phys. **141**, 114503 (2014).

[142]A. Zaragoza, M. A. Gonzales, L. Joly, I. López-Montero, M. A. Canales, A. L. Benavides, and C. Valeriani, "Molecular dynamics study of nanoconfined TIP4P/2005 water: how confinement and temperature affect diffusion and viscosity," Phys. Chem. Chem. Phys. **21**, 13653 (2019).

[143]G. S. Fanourgakis, J. S. Medina, and R. Prosmiti, "Determining the bulk viscosity of rigid water models," J. Phys. Chem. A **116**, 2564 (2012).

[144]G.-J. Guo, Y.-G. Zhang, K. Refson, and Y.-J. Zhao, "Viscosity and stress autocorrelation function in supercooled water: a molecular dynamics study," Mol. Phys. **100**, 2617 (2002).

[145]G. Delgado-Barrio, P. Villareal, G. Winter, J. S. Medina, B. González, J. V. Alemán, J. L. Gomez, P. Sangrá, J. J. Santana, and M. E. Torres, "Viscosity of liquid water via equilibrium molecular dynamics simulations," in *Frontiers in Quantum Systems in Chemistry and Physics*, edited by S. Wilson, P. J. Grout, G. Delgado-Barrio, and P. Piecuch (Springer, 2008) pp. 351–361.

[146]J. S. Medina, R. Prosmiti, P. Villarreal, G. Delgado-Barrio, G. Winter, B. González, J. V. Alemán, and C. Collado, "Molecular dynamics simulations of rigid and flexible water models: Temperature dependence of viscosity," Chem. Phys. **388**, 9 (2011).

[147]R. Kohlrausch, "Theorie des elektrischen Rückstandes in der Leidner Flasche," Ann. Phys. **167**, 179 (1854).

[148]G. Williams and D. C. Watts, "Non-symmetrical dielectric relaxation behaviour arising from a simple empirical decay function," Trans. Faraday Soc. **66**, 80 (1970).

[149]R. D. Mountain and R. Zwanig, "Shear relaxation times of simple fluids," J. Chem. Phys. **44**, 2777 (1966).

[150]T. A. Litovitz and C. M. Davis, "Structural and Shear Relaxation in Liquids," in *Peroperties of Gases, Liquids and Solutions*, Physical Acoustics, Vol. 2, edited by W. P. Mason (Academic Press, 1965) pp. 281–349.

[151]G. L. Murphy, "Big-Bang model without singularities," Phys. Rev. D **8**, 4231 (1973).

[152]V. A. Belinskii and I. M. Khalatnikov, "Influence of viscosity on the character of cosmological evolution," Zh. Eksp. Theor. Fiz. **69**, 401 (1975).

[153]I. Brevik, E. Elizalde, S. Nojiri, and S. D. Odintsov, "Viscous little rip cosmology," Phys. Rev. D **84**, 103508 (2011).

[154]R. Colistete, J. C. Fabris, J. Tossa, and W. Zimdahl, "Bulk viscous cosmology," Phys. Rev. D **76**, 103516 (2007).

[155]M. Cruz, N. Cruz, and S. Lepe, "Accerlerated and decelerated expansion in a causal dissipative cosmology," Phys. Rev. D **96**, 124020 (2017).

[156]B. Li and J. D. Barrow, "Does bulk viscosity create a viable unified dark matter model?" Phys. Rev. D **79**, 103521 (2009).

[157]S. R. deGroot and P. Mazur, *Non-Equilibrium Thermodynamics* (Dover, 1962).

[158]D. Jou, J. Casas-Vázquez, and G. Lebon, *Extended Irreversible Thermodynamics* (Springer, 2010).

[159]P. Borgelt, C. Hoheisel, and G. Stell, "Exact molecular dynamics and kinetic theory results for thermal transport coefficients of the Lennard-Jones argon fluid in a wide range of states," Phys. Rev. A **42**, 789 (1990).

[160]K. Tankeshwar, "Bulk viscosity and the relation between transport coefficients," Phys. Chem. Liq. **24**, 91 (1991).

TABLE III. Comparison of the bulk viscosity from the present equation of state (15) with literature data that have either been obtained by molecular dynamics simulation[140],[159] or by theoretical calculations[160].

T/T_c	p/p_c	ρ/ρ_c	$\mu_b\ \sigma^2/\sqrt{m\epsilon}$ Eq. (15)	$\mu_b\ \sigma^2/\sqrt{m\epsilon}$ literature
0.795	0.545	2.196	1.17	1.20 ± 0.37[140]
·	3.616	2.353	0.99	0.93 ± 0.05
·	8.727	2.510	0.92	0.87 ± 0.05
·	16.558	2.667	0.88	0.89 ± 0.05
0.875	1.118	2.039	1.42	1.10 ± 0.36
·	3.274	2.196	0.98	1.03 ± 0.05
·	6.966	2.353	0.79	0.79 ± 0.04
0.674	0.473	2.448	1.00	0.97 ± 0.10[159]
0.679	0.707	·	1.00	0.98 ± 0.10
0.826	7.875	·	0.89	0.75 ± 0.08
0.699	17.065	2.773	0.94	1.10 ± 0.11
0.763	21.558	·	0.91	1.00 ± 0.11
0.802	24.239	·	0.87	0.96 ± 0.10
0.605	3.117	2.640	0.96	1.05[160]
0.652	6.149	·	0.96	0.93
0.667	7.126	·	0.96	1.01
0.678	7.800	·	0.96	1.00
0.747	12.086	·	0.93	0.86
0.792	14.845	·	0.89	0.86

Supplementary material to: Bulk viscosity of liquid noble gases

René Spencer Chatwell and Jadran Vrabec[a)]

Thermodynamics and Process Engineering, Technische Universität Berlin, 10587 Berlin, Germany

All bulk viscosity data presented in the manuscript are disclosed in this supplementary material.

The bulk viscosity was computed from EMD simulations via improper time integration of the autocorrelation function of the microscopic stress tensor's diagonal elements [1]

$$\mu_b^{\chi\chi} = \frac{1}{Vk_BT}\int_0^\infty dt\langle\Big(J_p^{\chi\chi}(t) - pV(t)\Big)\cdot\Big(J_p^{\chi\chi}(0) - pV(0)\Big)\rangle \ , \tag{1}$$

where $\chi\chi = xx, yy$ and zz. Better statistics were achieved by considering the average value of all three independent spatial elements

$$\mu_b = \frac{1}{3}\sum \mu_b^{\chi\chi} \ . \tag{2}$$

The extended critical region was constructed on the basis of sound dispersion measurements from the literature. The discrepancy between the thermodynamic and frequency-dependent speed of sound, i.e. $c \neq c(\omega)$, delimits the extended critical region.

TABLE I. Critical data that were used to reduce temperature, pressure and density.

	T_c / K	p_c / MPa	ρ_c / mol/dm^3	Reference
Ne	44.40	2.662	24.10	[2]
Ar	150.69	4.863	13.41	[3]
Kr	209.48	5.525	10.85	[4]
Xe	289.73	5.842	8.40	[4]

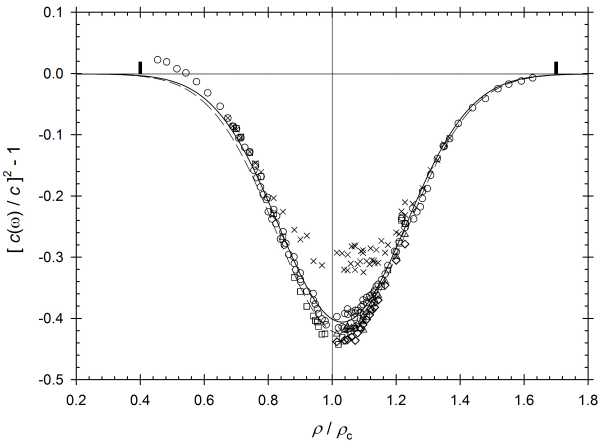

FIG. 1. Literature data of frequency-dependent speed of sound measurements in xenon along the saturated vapor and liquid lines. The frequencies were varied from $f = 0.4$ MHz (diamonds) [5], 0.55 MHz (triangles) [5], 0.6 MHz (squares) [6], 1 MHz (circles) [5, 6] to 3 MHz (crosses) [5, 6]. The squared ratio $\big(c(\omega)/c\big)^2$ was observed to follow a Gaussian function and is presented for $f = 0.55$ MHz (dashed) and 1 MHz (solid). The extended critical region was consequently found to be delimited to $\rho/\rho_c = 0.4$, $p/p_c = 0.738$ on the saturated vapor and $\rho/\rho_c = 1.70$, $p/p_c = 0.710$ on the saturated liquid line.

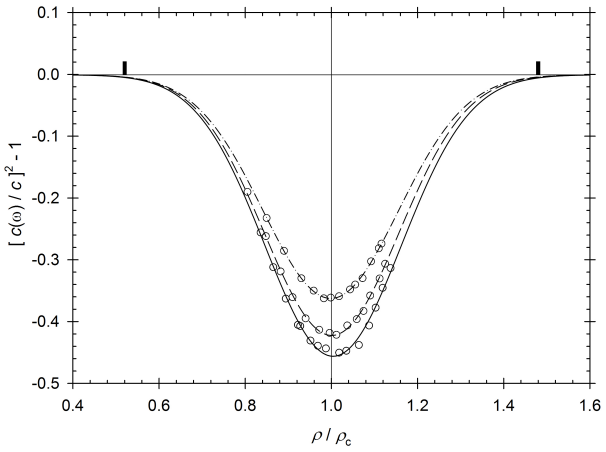

FIG. 2. Evaluation of additional xenon measurements [6] along the isotherms $T/T_c = 1.00009$ (solid), 1.00055 (dashed), 1.00113 (dash-dotted) at $f = 0.6$ MHz further confining the extended critical region between $\rho/\rho = 0.52$, $p/p_c = 0.933$ and $\rho/\rho_c = 1.13$, $p/p_c = 1.318$.

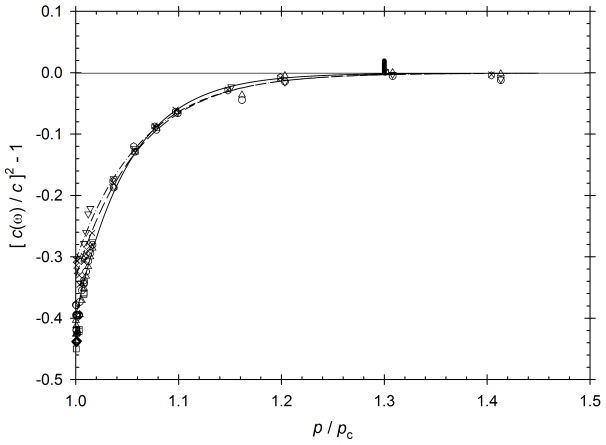

FIG. 3. Additional data along the critical isochore with the same symbols as in Fig. 1 with additional $f = 5$ MHz (inverted triangles) [5] and $f = 7$ MHz (hexaeders) [5] measurements. These results further confine the critical region to be at $p/p_c < 1.3$.

TABLE II. The critical region's boundary was constructed as a 4^{th}-order polynomial $g(x) = ax^4 + bx^3 + cx^2 + dx + e$. The parameters were fitted to the basis points indicated in Figs. 1 to 3, as summarized below, to yield $a = -0.8751$, $b = -0.2817$, $c = -0.9633$, $d = 0.2704$ and $e = 0.3$.

T/T_c	p/p_c	ρ/ρ_c
0.949	0.738	0.40
1.001	0.933	0.52
1.050	1.300	1.00
1.001	1.318	1.13
0.943	0.710	1.70

TABLE III: Overview of bulk viscosity data determined from experimental sound attenuation measurements from the literature for Neon [7].

T/T_c	p/p_c	ρ/ρ_c	f/μs	α_λ	$\Delta\alpha_\lambda$	$\mu^*_{b,\mathrm{exp.}}$	$\Delta\mu^*_{b,\mathrm{exp.}}$
0.55	0.041	2.568	30	0.00042	0.00002	1.49	1.09
0.55	0.028	2.568	30	0.00042	0.00002	1.52	1.10
0.55	0.022	2.567	30	0.00042	0.00002	1.51	1.10
0.55	0.017	2.567	30	0.00042	0.00002	1.51	1.09
0.57	0.149	2.553	30	0.00041	0.00002	1.41	1.05

TABLE III: continued

T/T_c	p/p_c	ρ/ρ_c	f/μs	α_λ	$\Delta\alpha_\lambda$	$\mu^*_{b,\mathrm{exp.}}$	$\Delta\mu^*_{b,\mathrm{exp.}}$
0.57	0.078	2.551	30	0.00041	0.00002	1.41	1.05
0.57	0.065	2.551	30	0.00041	0.00002	1.40	1.05
0.57	0.052	2.550	30	0.00041	0.00002	1.36	1.05
0.57	0.039	2.550	30	0.00042	0.00002	1.45	1.05
0.57	0.026	2.550	30	0.00042	0.00002	1.44	1.05
0.57	0.020	2.549	30	0.00042	0.00002	1.44	1.05
0.57	0.116	2.540	30	0.00041	0.00002	1.31	1.02
0.57	0.078	2.539	30	0.00041	0.00002	1.41	1.02
0.57	0.052	2.538	30	0.00042	0.00002	1.43	1.02
0.57	0.032	2.537	30	0.00042	0.00002	1.42	1.02
0.57	0.023	2.537	30	0.00042	0.00002	1.44	1.02
0.58	0.181	2.531	30	0.00040	0.00002	1.24	0.99
0.58	0.130	2.530	30	0.00040	0.00002	1.18	0.99
0.58	0.078	2.528	30	0.00040	0.00002	1.21	0.99
0.58	0.039	2.527	30	0.00040	0.00002	1.22	0.99
0.58	0.025	2.527	30	0.00041	0.00002	1.24	0.99
0.59	0.104	2.517	30	0.00042	0.00002	1.42	0.98
0.59	0.078	2.516	30	0.00042	0.00002	1.44	0.98
0.59	0.052	2.516	30	0.00042	0.00002	1.42	0.98
0.59	0.039	2.515	30	0.00042	0.00002	1.44	0.98
0.59	0.028	2.515	30	0.00042	0.00002	1.47	0.98
0.60	0.389	2.515	30	0.00043	0.00002	1.68	0.99
0.60	0.259	2.511	30	0.00043	0.00002	1.67	0.98
0.60	0.155	2.508	30	0.00042	0.00002	1.47	0.96
0.60	0.097	2.506	30	0.00044	0.00002	1.71	0.98
0.60	0.052	2.504	30	0.00042	0.00002	1.47	0.96
0.60	0.040	2.504	30	0.00041	0.00002	1.35	0.95
0.60	0.039	2.504	30	0.00043	0.00002	1.62	0.97
0.60	0.031	2.504	30	0.00042	0.00002	1.51	0.96
0.60	0.259	2.504	30	0.00042	0.00002	1.45	0.95
0.60	0.155	2.500	30	0.00042	0.00002	1.42	0.95
0.60	0.078	2.498	30	0.00042	0.00002	1.43	0.95
0.60	0.039	2.497	30	0.00042	0.00002	1.49	0.95
0.60	0.033	2.497	30	0.00042	0.00002	1.46	0.95
0.60	0.262	2.497	30	0.00044	0.00002	1.77	0.96
0.60	0.228	2.496	30	0.00044	0.00002	1.77	0.96
0.60	0.193	2.495	30	0.00044	0.00002	1.75	0.96
0.60	0.044	2.490	30	0.00044	0.00002	1.72	0.95
0.60	0.035	2.490	30	0.00044	0.00002	1.79	0.96
0.60	0.466	2.502	30	0.00043	0.00002	1.79	0.97
0.60	0.259	2.495	30	0.00044	0.00002	1.72	0.96
0.60	0.052	2.489	30	0.00044	0.00002	1.68	0.95
0.60	0.035	2.488	30	0.00044	0.00002	1.67	0.95
0.61	0.440	2.493	30	0.00040	0.00002	1.31	0.92
0.61	0.311	2.489	30	0.00040	0.00002	1.24	0.92
0.61	0.181	2.485	30	0.00041	0.00002	1.28	0.91
0.61	0.130	2.483	30	0.00041	0.00002	1.25	0.91
0.61	0.078	2.481	30	0.00041	0.00002	1.27	0.91
0.61	0.052	2.480	30	0.00041	0.00002	1.33	0.91
0.61	0.038	2.480	30	0.00041	0.00002	1.33	0.91
0.61	0.155	2.476	30	0.00042	0.00002	1.47	0.91
0.61	0.091	2.474	30	0.00042	0.00002	1.43	0.91
0.61	0.045	2.473	30	0.00043	0.00002	1.48	0.91
0.61	0.041	2.473	30	0.00043	0.00002	1.48	0.91

TABLE III: continued

T/T_c	p/p_c	ρ/ρ_c	f/μs	α_λ	$\Delta\alpha_\lambda$	$\mu^*_{b,\mathrm{exp.}}$	$\Delta\mu^*_{b,\mathrm{exp.}}$
0.62	0.570	2.480	30	0.00042	0.00002	1.51	0.91
0.62	0.389	2.475	30	0.00043	0.00002	1.56	0.91
0.62	0.207	2.469	30	0.00042	0.00002	1.43	0.90
0.62	0.104	2.465	30	0.00043	0.00002	1.57	0.90
0.62	0.052	2.463	30	0.00043	0.00002	1.56	0.90
0.62	0.044	2.463	30	0.00043	0.00002	1.55	0.90
0.63	0.155	2.456	30	0.00043	0.00002	1.56	0.89
0.63	0.104	2.454	30	0.00043	0.00002	1.55	0.89
0.63	0.052	2.453	30	0.00043	0.00002	1.47	0.88
0.63	0.048	2.452	30	0.00043	0.00002	1.49	0.88
0.63	0.928	2.472	30	0.00040	0.00002	1.39	0.89
0.63	0.440	2.456	30	0.00042	0.00002	1.42	0.88
0.63	0.311	2.452	30	0.00042	0.00002	1.34	0.87
0.63	0.181	2.447	30	0.00042	0.00002	1.31	0.86
0.63	0.130	2.446	30	0.00042	0.00002	1.35	0.86
0.63	0.078	2.444	30	0.00042	0.00002	1.32	0.86
0.63	0.051	2.443	30	0.00042	0.00002	1.30	0.86
0.64	0.389	2.446	30	0.00044	0.00002	1.63	0.88
0.64	0.233	2.441	30	0.00043	0.00002	1.51	0.86
0.64	0.104	2.436	30	0.00044	0.00002	1.49	0.86
0.64	0.065	2.434	30	0.00043	0.00002	1.47	0.86
0.64	0.055	2.434	30	0.00043	0.00002	1.46	0.85
0.65	1.036	2.456	30	0.00041	0.00002	1.51	0.87
0.65	0.259	2.429	30	0.00043	0.00002	1.45	0.84
0.65	0.130	2.425	30	0.00043	0.00002	1.45	0.84
0.65	0.065	2.422	30	0.00044	0.00002	1.43	0.84
0.65	0.059	2.422	30	0.00044	0.00002	1.43	0.84
0.65	0.999	2.445	30	0.00043	0.00002	1.68	0.87
0.65	0.780	2.438	30	0.00042	0.00002	1.45	0.85
0.65	0.505	2.428	30	0.00043	0.00002	1.47	0.84
0.65	0.262	2.419	30	0.00043	0.00002	1.40	0.83
0.65	0.079	2.412	30	0.00044	0.00002	1.41	0.82
0.65	0.078	2.412	30	0.00046	0.00002	1.69	0.84
0.65	0.076	2.412	30	0.00043	0.00002	1.35	0.82
0.65	0.064	2.412	30	0.00044	0.00002	1.40	0.82
0.67	0.518	2.405	30	0.00043	0.00002	1.45	0.81
0.67	0.337	2.398	30	0.00045	0.00002	1.52	0.81
0.67	0.233	2.394	30	0.00045	0.00002	1.49	0.81
0.67	0.130	2.390	30	0.00045	0.00002	1.52	0.80
0.67	0.078	2.388	30	0.00045	0.00002	1.52	0.80
0.67	0.074	2.388	30	0.00045	0.00002	1.52	0.80
0.67	1.026	2.420	30	0.00044	0.00002	1.72	0.84
0.67	0.518	2.401	30	0.00044	0.00002	1.56	0.81
0.67	0.130	2.386	30	0.00045	0.00002	1.48	0.80
0.67	0.077	2.383	30	0.00045	0.00002	1.46	0.79
0.68	1.036	2.407	30	0.00043	0.00002	1.55	0.81
0.68	0.933	2.404	30	0.00043	0.00002	1.46	0.81
0.68	0.674	2.394	30	0.00043	0.00002	1.38	0.79
0.68	0.415	2.383	30	0.00044	0.00002	1.39	0.79
0.68	0.285	2.378	30	0.00044	0.00002	1.38	0.78
0.68	0.155	2.373	30	0.00045	0.00002	1.38	0.78
0.68	0.104	2.370	30	0.00045	0.00002	1.38	0.78
0.68	0.084	2.370	30	0.00045	0.00002	1.39	0.78
0.69	1.009	2.379	30	0.00044	0.00002	1.53	0.78

TABLE III: continued

T/T_c	p/p_c	ρ/ρ_c	f/μs	α_λ	$\Delta\alpha_\lambda$	$\mu^*_{b,\mathrm{exp.}}$	$\Delta\mu^*_{b,\mathrm{exp.}}$
0.69	0.780	2.369	30	0.00045	0.00002	1.51	0.78
0.69	0.500	2.358	30	0.00045	0.00002	1.45	0.76
0.69	0.262	2.347	30	0.00045	0.00002	1.27	0.75
0.69	0.107	2.340	30	0.00047	0.00002	1.43	0.75
0.69	0.101	2.340	30	0.00047	0.00002	1.44	0.75
0.71	1.023	2.349	30	0.00046	0.00002	1.59	0.76
0.71	0.777	2.338	30	0.00046	0.00002	1.53	0.75
0.71	0.518	2.327	30	0.00048	0.00002	1.55	0.74
0.71	0.259	2.315	30	0.00049	0.00002	1.55	0.73
0.71	0.130	2.308	30	0.00050	0.00002	1.53	0.73
0.71	0.120	2.308	30	0.00050	0.00002	1.52	0.73
0.73	1.036	2.319	30	0.00047	0.00002	1.56	0.73
0.73	0.777	2.306	30	0.00048	0.00002	1.55	0.72
0.73	0.518	2.294	30	0.00049	0.00002	1.51	0.71
0.73	0.259	2.280	30	0.00051	0.00002	1.55	0.71
0.73	0.155	2.275	30	0.00053	0.00002	1.62	0.71
0.73	0.143	2.274	30	0.00053	0.00002	1.59	0.71
0.75	1.035	2.287	30	0.00049	0.00002	1.53	0.70
0.75	0.905	2.281	30	0.00048	0.00002	1.42	0.69
0.75	0.719	2.271	30	0.00050	0.00002	1.52	0.69
0.75	0.506	2.259	30	0.00051	0.00002	1.45	0.68
0.75	0.312	2.248	30	0.00053	0.00002	1.53	0.68
0.75	0.181	2.241	30	0.00053	0.00002	1.46	0.67
0.75	0.168	2.240	30	0.00054	0.00002	1.50	0.68
0.76	1.036	2.252	30	0.00051	0.00002	1.57	0.68
0.76	0.777	2.238	30	0.00053	0.00002	1.59	0.68
0.76	0.518	2.223	30	0.00056	0.00002	1.64	0.67
0.76	0.311	2.210	30	0.00058	0.00002	1.62	0.66
0.76	0.207	2.203	30	0.00059	0.00002	1.66	0.66
0.76	0.197	2.202	30	0.00059	0.00002	1.65	0.66
0.78	1.036	2.217	30	0.00054	0.00002	1.56	0.66
0.78	1.009	2.215	30	0.00053	0.00002	1.43	0.65
0.78	0.779	2.201	30	0.00056	0.00002	1.56	0.65
0.78	0.777	2.201	30	0.00056	0.00002	1.54	0.65
0.78	0.518	2.184	30	0.00059	0.00002	1.57	0.64
0.78	0.491	2.182	30	0.00057	0.00002	1.46	0.64
0.78	0.338	2.171	30	0.00061	0.00002	1.64	0.64
0.78	0.246	2.165	30	0.00061	0.00002	1.51	0.63
0.78	0.230	2.163	30	0.00062	0.00002	1.55	0.63
0.81	1.036	2.157	30	0.00060	0.00002	1.66	0.63
0.81	0.777	2.138	30	0.00064	0.00003	1.68	0.62
0.81	0.518	2.117	30	0.00067	0.00003	1.67	0.61
0.81	0.298	2.098	30	0.00073	0.00003	1.79	0.61
0.81	0.290	2.097	30	0.00073	0.00003	1.77	0.61
0.84	1.036	2.101	30	0.00067	0.00003	1.69	0.61
0.84	0.777	2.079	30	0.00071	0.00003	1.72	0.60
0.84	0.518	2.054	30	0.00078	0.00003	1.78	0.59
0.84	0.363	2.038	30	0.00082	0.00003	1.81	0.59
0.84	0.351	2.034	30	0.00083	0.00003	1.81	0.59

TABLE IV: Bulk viscosity data determined from experimental sound attenuation measurements from the literature for argon [8].

T/T_c	p/p_c	ρ/ρ_c	f/μs	α_λ	$\Delta\alpha_\lambda$	$\mu^*_{b,\mathrm{exp.}}$	$\Delta\mu^*_{b,\mathrm{exp.}}$
0.56	0.014	2.645	42	0.00053	0.00002	1.80	1.38
0.56	0.014	2.643	42	0.00053	0.00002	1.79	1.38
0.56	0.016	2.632	42	0.00053	0.00002	1.73	1.35
0.57	0.018	2.620	42	0.00053	0.00002	1.71	1.32
0.58	0.022	2.597	42	0.00052	0.00002	1.62	1.27
0.60	0.027	2.574	42	0.00052	0.00002	1.53	1.22
0.62	0.037	2.539	42	0.00053	0.00002	1.46	1.15
0.63	0.044	2.515	42	0.00053	0.00002	1.45	1.12
0.64	0.052	2.490	42	0.00055	0.00002	1.51	1.09

TABLE V: Bulk viscosity data determined from experimental sound attenuation measurements from the literature for argon [9].

T/T_c	p/p_c	ρ/ρ_c	f/μs	α_λ	$\Delta\alpha_\lambda$	$\mu^*_{b,\mathrm{exp.}}$	$\Delta\mu^*_{b,\mathrm{exp.}}$
0.57	1.153	2.645	50	0.00062	0.00002	1.91	1.38
0.58	1.596	2.641	50	0.00063	0.00002	2.10	1.39
0.59	1.875	2.642	50	0.00063	0.00002	2.23	1.40
0.59	2.276	2.642	50	0.00061	0.00002	2.02	1.38
0.60	2.720	2.642	50	0.00058	0.00002	1.69	1.34
0.60	3.130	2.641	50	0.00058	0.00002	1.84	1.35
0.58	1.333	2.634	50	0.00064	0.00002	2.19	1.39
0.59	1.576	2.634	50	0.00063	0.00002	2.15	1.38
0.59	1.976	2.635	50	0.00061	0.00002	2.00	1.36
0.60	2.744	2.634	50	0.00061	0.00002	2.02	1.36
0.61	3.129	2.634	50	0.00059	0.00002	1.90	1.34
0.56	0.562	2.645	50	0.00067	0.00002	2.38	1.44
0.58	0.948	2.635	50	0.00063	0.00002	1.99	1.37
0.58	1.310	2.634	50	0.00062	0.00002	1.87	1.35
0.59	1.593	2.635	50	0.00061	0.00002	1.85	1.35
0.59	1.833	2.634	50	0.00060	0.00002	1.74	1.34
0.60	2.275	2.632	50	0.00059	0.00002	1.73	1.33
0.60	2.501	2.634	50	0.00059	0.00002	1.80	1.34
0.61	3.005	2.632	50	0.00058	0.00002	1.70	1.32
0.58	0.384	2.622	50	0.00071	0.00002	2.72	1.42
0.58	0.705	2.619	50	0.00071	0.00002	2.78	1.42
0.59	1.170	2.619	50	0.00070	0.00002	2.83	1.42
0.59	1.291	2.617	50	0.00069	0.00002	2.74	1.41
0.60	1.994	2.621	50	0.00068	0.00002	2.72	1.40
0.71	1.393	2.421	50	0.00068	0.00002	1.64	0.88
0.72	1.752	2.416	50	0.00067	0.00002	1.61	0.87
0.72	2.140	2.418	50	0.00066	0.00002	1.57	0.87
0.73	2.521	2.414	50	0.00064	0.00002	1.48	0.86
0.75	2.985	2.413	50	0.00064	0.00002	1.56	0.86
0.75	3.125	2.415	50	0.00063	0.00002	1.51	0.86
0.68	0.264	2.420	50	0.00075	0.00003	1.92	0.91
0.70	0.866	2.420	50	0.00072	0.00003	1.84	0.90
0.70	1.270	2.423	50	0.00070	0.00002	1.79	0.90
0.72	1.933	2.418	50	0.00068	0.00002	1.68	0.88
0.73	2.461	2.418	50	0.00067	0.00002	1.69	0.88
0.75	3.146	2.415	50	0.00064	0.00002	1.59	0.86
0.70	0.808	2.412	50	0.00071	0.00002	1.65	0.87
0.72	1.837	2.410	50	0.00064	0.00002	1.33	0.84
0.73	2.401	2.413	50	0.00064	0.00002	1.48	0.85

TABLE V: continued

T/T_c	p/p_c	ρ/ρ_c	f/μs	α_λ	$\Delta\alpha_\lambda$	$\mu^*_{b,\mathrm{exp.}}$	$\Delta\mu^*_{b,\mathrm{exp.}}$
0.74	2.400	2.409	50	0.00064	0.00002	1.43	0.85
0.75	2.744	2.404	50	0.00064	0.00002	1.45	0.84
0.75	3.164	2.404	50	0.00062	0.00002	1.37	0.83
0.70	0.645	2.398	50	0.00087	0.00003	2.75	0.97
0.72	1.551	2.397	50	0.00082	0.00003	2.63	0.96
0.74	2.078	2.395	50	0.00080	0.00003	2.57	0.95
0.75	2.542	2.393	50	0.00077	0.00003	2.36	0.93
0.76	3.143	2.391	50	0.00075	0.00003	2.36	0.92
0.87	0.545	1.985	30	0.00106	0.00004	2.52	0.73
0.89	1.150	1.997	30	0.00089	0.00003	2.12	0.70
0.92	1.835	2.003	30	0.00078	0.00003	1.87	0.67
0.95	2.561	1.999	30	0.00073	0.00003	1.84	0.67
0.96	3.084	2.000	30	0.00068	0.00002	1.68	0.65
0.87	0.524	1.982	30	0.00106	0.00004	2.47	0.72
0.89	0.949	1.989	30	0.00096	0.00003	2.31	0.71
0.90	1.250	1.989	30	0.00090	0.00003	2.15	0.69
0.93	2.178	1.995	30	0.00080	0.00003	2.08	0.69
0.95	2.541	1.997	30	0.00077	0.00003	2.07	0.69
0.97	3.185	1.997	30	0.00075	0.00003	2.12	0.69

TABLE VI: Bulk viscosity data determined from experimental sound attenuation measurements from the literature for argon [10].

T/T_c	p/p_c	ρ/ρ_c	f/μs	α_λ	$\Delta\alpha_\lambda$	$\mu^*_{b,\mathrm{exp.}}$	$\Delta\mu^*_{b,\mathrm{exp.}}$
0.60	0.027	2.574	55	0.00070	0.00002	1.68	1.17
0.60	0.417	2.585	55	0.00069	0.00002	1.70	1.19
0.60	0.833	2.596	55	0.00068	0.00002	1.69	1.21
0.60	1.250	2.607	55	0.00066	0.00002	1.67	1.22
0.66	0.067	2.453	55	0.00077	0.00002	1.71	0.87
0.66	0.417	2.466	55	0.00075	0.00002	1.66	0.87
0.66	0.834	2.480	55	0.00072	0.00002	1.59	0.88
0.66	1.250	2.494	55	0.00069	0.00002	1.54	0.88
0.73	0.137	2.320	55	0.00089	0.00003	1.64	0.77
0.73	0.417	2.334	55	0.00086	0.00003	1.60	0.77
0.73	0.834	2.354	55	0.00082	0.00002	1.58	0.78
0.73	1.250	2.373	55	0.00079	0.00002	1.62	0.80
0.80	0.249	2.171	55	0.00116	0.00003	1.75	0.69
0.80	0.417	2.184	55	0.00111	0.00003	1.72	0.70
0.80	0.833	2.212	55	0.00102	0.00003	1.67	0.71
0.80	1.250	2.238	55	0.00095	0.00003	1.63	0.72
0.86	0.417	1.994	55	0.00178	0.00007	2.12	0.73
0.86	0.834	2.043	55	0.00144	0.00006	1.84	0.73
0.86	1.042	2.064	55	0.00131	0.00005	1.71	0.72
0.86	1.250	2.083	55	0.00122	0.00005	1.63	0.72
0.90	0.525	1.889	55	0.00243	0.00010	2.43	0.72
0.90	0.833	1.940	55	0.00189	0.00008	2.09	0.71
0.90	1.042	1.968	55	0.00166	0.00007	1.91	0.70
0.90	1.250	1.993	55	0.00149	0.00006	1.74	0.69
0.93	0.651	1.762	55	0.00403	0.00016	3.33	0.77
0.93	0.833	1.811	55	0.00306	0.00012	2.86	0.74
0.93	1.042	1.855	55	0.00233	0.00009	2.27	0.69
0.93	1.250	1.890	55	0.00196	0.00008	2.00	0.68

TABLE VI: continued

T/T_c	p/p_c	ρ/ρ_c	f/μs	α_λ	$\Delta\alpha_\lambda$	$\mu^*_{b,\mathrm{exp.}}$	$\Delta\mu^*_{b,\mathrm{exp.}}$
0.96	0.800	1.595	25	0.00413	0.00025	5.24	1.17
0.96	0.833	1.617	35	0.00431	0.00026	3.99	1.00
0.96	1.042	1.707	55	0.00366	0.00015	2.61	0.68
0.96	1.250	1.764	55	0.00269	0.00011	2.13	0.65
1.00	1.042	1.447	25	0.00591	0.00065	5.23	1.73
1.00	1.146	1.538	35	0.00432	0.00026	3.48	0.90
1.00	1.250	1.594	35	0.00305	0.00012	2.76	0.66

TABLE VII: Bulk viscosity data determined from experimental sound attenuation measurements from the literature for argon [11].

T/T_c	p/p_c	ρ/ρ_c	f/μs	α_λ	$\Delta\alpha_\lambda$	$\mu^*_{b,\mathrm{exp.}}$	$\Delta\mu^*_{b,\mathrm{exp.}}$
0.93	0.644	1.762	55	0.00450	0.00027	3.96	1.05
0.93	0.720	1.782	55	0.00371	0.00022	3.31	0.97
0.93	0.823	1.809	55	0.00318	0.00019	3.00	0.94
0.93	0.925	1.832	55	0.00282	0.00017	2.80	0.92
0.95	0.731	1.669	55	0.00652	0.00039	4.59	1.10
0.96	0.791	1.595	55	0.01000	0.00060	5.95	1.27
0.96	0.823	1.610	55	0.00795	0.00048	4.80	1.11
0.96	0.884	1.644	55	0.00615	0.00037	4.09	1.02
0.96	1.028	1.702	55	0.00399	0.00024	2.94	0.89
0.96	1.234	1.761	55	0.00296	0.00018	2.49	0.85
0.98	0.874	1.513	55	0.01287	0.00077	5.82	1.22
0.98	0.925	1.560	55	0.00910	0.00055	4.90	1.11
0.98	1.028	1.621	55	0.00564	0.00034	3.52	0.94
0.98	1.234	1.699	55	0.00343	0.00021	2.47	0.82
0.99	1.028	1.543	55	0.00850	0.00051	4.49	1.04
0.99	1.234	1.647	55	0.00413	0.00025	2.70	0.83
0.99	1.028	1.474	55	0.01209	0.00073	5.28	1.13
0.99	1.090	1.528	55	0.00809	0.00049	4.12	0.99
0.99	1.234	1.608	55	0.00481	0.00029	2.93	0.85
1.00	1.028	1.429	55	0.01488	0.00164	5.64	1.81
1.00	1.131	1.528	55	0.00760	0.00046	3.89	0.96
1.00	1.234	1.586	55	0.00532	0.00032	3.14	0.87

TABLE VIII: Bulk viscosity data determined from experimental sound attenuation measurements from the literature for argon [12].

T/T_c	p/p_c	ρ/ρ_c	f/μs	α_λ	$\Delta\alpha_\lambda$	$\mu^*_{b,\mathrm{exp.}}$	$\Delta\mu^*_{b,\mathrm{exp.}}$
0.56	0.167	2.647	62.5	0.00079	0.00005	0.34	1.74
0.58	0.167	2.613	62.5	0.00076	0.00005	0.34	1.60
0.60	0.167	2.578	62.5	0.00077	0.00005	0.35	1.51
0.74	0.167	2.293	62.5	0.00109	0.00007	0.51	1.07

TABLE IX: Bulk viscosity data determined from experimental sound attenuation measurements from the literature for argon [13].

T/T_c	p/p_c	ρ/ρ_c	f/μs	α_λ	$\Delta\alpha_\lambda$	$\mu^*_{b,\mathrm{exp.}}$	$\Delta\mu^*_{b,\mathrm{exp.}}$
1.01	1.168	1.429	5	0.00166	0.00018	8.46	2.66
1.04	1.245	0.981	5	0.00322	0.00035	6.21	1.96
1.04	1.251	1.000	5	0.00337	0.00037	6.79	2.10
1.04	1.257	1.023	5	0.00339	0.00037	7.17	2.20
1.04	1.273	1.073	5	0.00318	0.00035	7.40	2.27
1.06	1.333	0.910	5	0.00161	0.00018	2.63	1.08
1.06	1.351	0.952	5	0.00170	0.00019	3.08	1.20
1.06	1.365	0.985	5	0.00182	0.00020	3.62	1.34
1.06	1.371	1.000	5	0.00187	0.00021	3.87	1.41
1.06	1.377	1.012	5	0.00185	0.00020	3.90	1.42
1.06	1.389	1.039	5	0.00178	0.00020	3.96	1.44
1.06	1.412	1.087	5	0.00174	0.00019	4.34	1.55

TABLE X: Bulk viscosity data determined from experimental sound attenuation measurements from the literature for krypton [14].

T/T_c	p/p_c	ρ/ρ_c	f/μs	α_λ	$\Delta\alpha_\lambda$	$\mu^*_{b,\mathrm{exp.}}$	$\Delta\mu^*_{b,\mathrm{exp.}}$
0.57	0.019	2.656	55	0.00091	0.00004	1.30	1.78
0.57	0.362	2.665	55	0.00091	0.00004	1.37	1.81
0.57	0.724	2.674	55	0.00090	0.00004	1.42	1.84
0.57	0.905	2.679	55	0.00090	0.00004	1.45	1.86
0.57	1.177	2.686	55	0.00089	0.00004	1.49	1.88
0.67	0.070	2.479	55	0.00102	0.00004	1.31	1.25
0.67	0.362	2.490	55	0.00100	0.00004	1.35	1.27
0.67	0.724	2.504	55	0.00097	0.00004	1.37	1.29
0.67	0.905	2.510	55	0.00096	0.00004	1.37	1.30
0.67	1.176	2.520	55	0.00095	0.00004	1.41	1.32
0.72	0.119	2.382	55	0.00114	0.00005	1.36	1.08
0.72	0.181	2.385	55	0.00110	0.00004	1.19	1.07
0.72	0.362	2.394	55	0.00105	0.00004	1.08	1.08
0.72	0.724	2.411	55	0.00101	0.00004	1.06	1.10
0.72	0.905	2.419	55	0.00098	0.00004	1.04	1.11
0.72	1.176	2.431	55	0.00097	0.00004	1.07	1.13
0.76	0.188	2.277	55	0.00135	0.00005	1.47	0.95
0.81	0.282	2.162	55	0.00169	0.00007	1.66	0.85
0.86	0.405	2.030	55	0.00236	0.00009	2.03	0.77
0.86	0.543	2.047	55	0.00213	0.00009	1.81	0.76
0.86	0.724	2.068	55	0.00192	0.00008	1.62	0.77
0.86	0.905	2.087	55	0.00179	0.00007	1.57	0.78
0.86	1.176	2.113	55	0.00164	0.00007	1.49	0.79
0.91	0.564	1.872	55	0.00388	0.00016	2.68	0.71
0.91	0.724	1.905	55	0.00330	0.00013	2.47	0.71
0.91	0.905	1.936	55	0.00280	0.00011	2.19	0.71
0.91	1.086	1.963	55	0.00247	0.00010	2.00	0.72
0.91	1.176	1.976	55	0.00232	0.00009	1.89	0.72
0.93	0.658	1.776	5	0.00054	0.00002	3.58	0.71
0.93	0.724	1.796	5	0.00047	0.00002	3.28	0.70
0.93	0.905	1.843	5	0.00034	0.00001	2.49	0.68
0.93	1.086	1.879	5	0.00028	0.00001	2.14	0.68
0.93	1.176	1.895	5	0.00026	0.00001	2.07	0.68
0.96	1.218	1.795	5	0.00039	0.00002	2.89	0.68
0.96	0.938	1.712	5	0.00056	0.00002	3.25	0.66
0.96	0.854	1.677	5	0.00083	0.00003	4.81	0.74

TABLE X: continued

T/T_c	p/p_c	ρ/ρ_c	f/μs	α_λ	$\Delta\alpha_\lambda$	$\mu^*_{b,\mathrm{exp.}}$	$\Delta\mu^*_{b,\mathrm{exp.}}$
0.96	0.781	1.637	5	0.00112	0.00004	5.64	0.77
0.97	1.267	1.761	5	0.00044	0.00003	3.16	0.78
0.97	1.021	1.681	5	0.00068	0.00004	4.04	0.81
0.97	0.872	1.602	5	0.00138	0.00008	6.81	1.00
0.97	0.832	1.570	5	0.00179	0.00020	7.84	1.55
0.98	1.238	1.681	5	0.00054	0.00003	3.19	0.75
0.98	1.079	1.612	5	0.00100	0.00006	5.37	0.89
0.98	1.037	1.587	5	0.00117	0.00007	5.83	0.92
0.98	0.970	1.536	5	0.00180	0.00011	7.63	1.04
0.99	1.234	1.638	5	0.00063	0.00004	3.34	0.74
0.99	1.061	1.540	5	0.00140	0.00008	6.10	0.92
0.99	1.005	1.484	5	0.00246	0.00015	9.23	1.15
0.99	0.972	1.435	5	0.00386	0.00023	12.22	1.38
0.99	0.952	1.385	5	0.00721	0.00079	19.49	3.01

TABLE XI: Bulk viscosity data determined from experimental sound attenuation measurements from the literature for krypton [15].

T/T_c	p/p_c	ρ/ρ_c	f/μs	α_λ	$\Delta\alpha_\lambda$	$\mu^*_{b,\mathrm{exp.}}$	$\Delta\mu^*_{b,\mathrm{exp.}}$
0.91	0.564	1.872	7.5	0.0006	0.00004	2.99	0.94
0.91	0.564	1.872	10	0.0007	0.00006	2.87	0.93
0.91	0.564	1.872	15	0.0011	0.00009	2.94	0.93
0.93	0.658	1.776	5	0.0008	0.00006	6.33	1.22
0.93	0.658	1.776	7.5	0.0008	0.00007	3.76	0.96
0.93	0.658	1.776	10	0.0011	0.00007	3.73	0.84
0.93	0.658	1.776	15	0.0016	0.00010	3.67	0.83
0.95	0.763	1.658	5	0.0011	0.00008	5.71	1.09
0.95	0.763	1.658	7.5	0.0015	0.00009	5.18	0.89
0.95	0.763	1.658	10	0.0021	0.00012	5.54	0.92
0.95	0.763	1.658	15	0.0031	0.00018	5.51	0.92
0.96	0.781	1.637	5	0.0012	0.00009	5.93	1.10
0.96	0.781	1.637	15	0.0034	0.00021	5.85	0.94
0.96	0.809	1.602	5	0.0015	0.00012	7.00	1.19
0.96	0.809	1.602	7.5	0.0022	0.00013	6.80	1.00
0.97	0.832	1.570	5	0.0020	0.00016	8.92	1.37
0.97	0.832	1.570	7.5	0.0030	0.00018	8.86	1.16
0.97	0.832	1.570	10	0.0040	0.00024	8.84	1.15
0.97	0.832	1.570	15	0.0056	0.00033	8.17	1.10
1.04	1.212	1.000	5	0.0053	0.00042	10.42	1.34
1.04	1.212	1.000	7.5	0.0074	0.00044	9.60	1.04
1.04	1.212	1.000	10	0.0090	0.00054	8.74	0.97
1.04	1.227	1.000	5	0.0046	0.00037	9.12	1.21
1.04	1.227	1.000	10	0.0081	0.00049	7.95	0.91
1.04	1.241	1.000	5	0.0041	0.00033	8.16	1.11
1.04	1.241	1.000	7.5	0.0060	0.00036	8.00	0.91
1.04	1.241	1.000	10	0.0076	0.00046	7.50	0.87
1.04	1.255	1.000	5	0.00373	0.00030	7.45	1.04
1.04	1.255	1.000	10	0.00693	0.00042	6.85	0.82
1.05	1.269	1.000	5	0.00353	0.00028	7.14	1.01
1.05	1.269	1.000	10	0.00632	0.00038	6.28	0.77

TABLE XII: Bulk viscosity data determined from experimental sound attenuation measurements from the literature for xenon [15].

T/T_c	p/p_c	ρ/ρ_c	f/μs	α_λ	$\Delta\alpha_\lambda$	$\mu^*_{b,\mathrm{exp.}}$	$\Delta\mu^*_{b,\mathrm{exp.}}$
0.56	0.014	2.689	42	0.000740	0.00003	1.34	0.68
0.56	0.015	2.686	42	0.000739	0.00003	1.33	0.68
0.56	0.015	2.680	42	0.000739	0.00003	1.31	0.67
0.57	0.017	2.668	42	0.000740	0.00003	1.28	0.66
0.59	0.023	2.637	42	0.000748	0.00003	1.25	0.63
0.60	0.030	2.606	42	0.000775	0.00003	1.35	0.61
0.62	0.038	2.575	42	0.000837	0.00003	1.67	0.60

TABLE XIII: Bulk viscosity data determined from experimental sound attenuation measurements from the literature for xenon [8].

T/T_c	p/p_c	ρ/ρ_c	f/μs	α_λ	$\Delta\alpha_\lambda$	$\mu^*_{b,\mathrm{exp.}}$	$\Delta\mu^*_{b,\mathrm{exp.}}$
0.57	0.017	2.668	55	0.001100	0.00004	2.16	0.74
0.57	0.145	2.671	55	0.001094	0.00004	2.16	0.75
0.57	0.501	2.680	55	0.001088	0.00004	2.25	0.76
0.57	0.868	2.689	55	0.001078	0.00004	2.30	0.77
0.57	1.132	2.696	55	0.001072	0.00004	2.34	0.78
0.59	0.023	2.637	55	0.001104	0.00004	2.04	0.71
0.60	0.030	2.606	55	0.001096	0.00004	1.84	0.67
0.62	0.038	2.575	55	0.001090	0.00004	1.64	0.63
0.62	0.098	2.577	55	0.001082	0.00004	1.62	0.63
0.62	0.449	2.588	55	0.001077	0.00004	1.72	0.64
0.62	0.782	2.598	55	0.001084	0.00004	1.88	0.66
0.62	1.113	2.606	55	0.001060	0.00004	1.83	0.66
0.69	0.089	2.442	55	0.001247	0.00005	1.63	0.54
0.69	0.098	2.443	55	0.001226	0.00005	1.55	0.54
0.69	0.401	2.455	55	0.001177	0.00005	1.48	0.54
0.69	0.741	2.469	55	0.001139	0.00005	1.46	0.55
0.69	1.002	2.479	55	0.001116	0.00004	1.46	0.55
0.74	0.152	2.334	55	0.001472	0.00006	1.76	0.50
0.76	0.179	2.295	55	0.001581	0.00006	1.83	0.49
0.76	0.264	2.300	55	0.001516	0.00006	1.69	0.48
0.76	0.417	2.309	55	0.001460	0.00006	1.61	0.48
0.76	0.757	2.328	55	0.001365	0.00005	1.51	0.48
0.76	1.015	2.342	55	0.001300	0.00005	1.43	0.48
0.78	0.209	2.255	55	0.001683	0.00007	1.83	0.47
0.83	0.320	2.125	55	0.002178	0.00009	1.97	0.44
0.83	0.436	2.136	55	0.002019	0.00008	1.77	0.43
0.83	0.607	2.152	55	0.001904	0.00008	1.71	0.43
0.83	0.767	2.165	55	0.001801	0.00007	1.62	0.43
0.83	0.996	2.183	55	0.001684	0.00007	1.54	0.43
0.86	0.415	2.027	55	0.002903	0.00012	2.39	0.43
0.88	0.469	1.973	55	0.003296	0.00013	2.43	0.42
0.90	0.528	1.914	55	0.004078	0.00016	2.80	0.43
0.90	0.634	1.934	55	0.003257	0.00013	2.07	0.39
0.90	0.807	1.962	55	0.002927	0.00012	2.01	0.39
0.90	0.972	1.986	55	0.002674	0.00011	1.94	0.40
0.90	1.055	1.997	55	0.002555	0.00010	1.88	0.40
0.91	0.592	1.851	55	0.005305	0.00021	3.32	0.45
0.91	0.637	1.861	55	0.004415	0.00018	2.60	0.41
0.91	0.816	1.899	55	0.003664	0.00015	2.36	0.40
0.91	0.976	1.927	55	0.003174	0.00013	2.13	0.39
0.91	1.051	1.939	55	0.002982	0.00012	2.02	0.39

TABLE XIII: continued

T/T_c	p/p_c	ρ/ρ_c	f/μs	α_λ	$\Delta\alpha_\lambda$	$\mu^*_{b,\mathrm{exp.}}$	$\Delta\mu^*_{b,\mathrm{exp.}}$
0.93	0.661	1.779	5	0.000757	0.00002	4.86	0.39
0.93	0.661	1.779	7.5	0.001094	0.00002	4.61	0.38
0.93	0.661	1.779	10	0.001544	0.00009	5.00	0.68
0.93	0.672	1.783	55	0.006304	0.00025	3.28	0.43
0.93	0.672	1.783	5	0.000716	0.00008	4.59	0.97
0.93	0.822	1.825	55	0.004724	0.00019	2.66	0.40
0.93	0.822	1.825	5	0.000514	0.00006	3.59	0.85
0.93	0.984	1.861	55	0.003883	0.00016	2.35	0.39
0.93	1.067	1.878	55	0.003536	0.00014	2.18	0.39
0.93	1.067	1.878	5	0.000392	0.00004	3.13	0.81
0.95	0.737	1.697	55	0.011588	0.00127	5.45	1.06
0.95	0.737	1.697	5	0.001181	0.00013	6.33	1.18
0.95	0.737	1.697	7.5	0.001643	0.00018	5.74	1.10
0.95	0.737	1.697	10	0.002201	0.00013	5.77	0.72
0.95	0.846	1.742	55	0.006755	0.00027	3.28	0.42
0.95	0.846	1.742	5	0.000745	0.00008	4.39	0.94
0.95	1.001	1.789	55	0.004943	0.00020	2.63	0.39
0.95	1.001	1.789	5	0.000543	0.00006	3.59	0.85
0.95	1.084	1.810	55	0.004366	0.00017	2.40	0.38
0.95	1.084	1.810	5	0.000494	0.00005	3.48	0.84
0.96	0.793	1.629	5	0.001780	0.00020	8.06	1.39
0.96	0.793	1.629	7.5	0.002483	0.00027	7.38	1.30
0.96	0.793	1.629	10	0.003492	0.00038	7.87	1.36
0.96	0.856	1.666	5	0.001212	0.00013	6.12	1.14
0.96	1.027	1.735	5	0.000726	0.00008	4.47	0.95
0.96	1.113	1.761	5	0.000653	0.00007	4.41	0.95
0.97	0.844	1.561	5	0.003015	0.00033	11.44	1.82
0.97	0.844	1.561	7.5	0.004186	0.00046	10.47	1.69
0.97	0.844	1.561	10	0.005929	0.00065	11.22	1.79
0.97	0.941	1.632	5	0.001188	0.00013	5.41	1.04
0.97	1.027	1.674	5	0.000955	0.00011	5.08	1.01
0.97	1.113	1.707	5	0.000881	0.00010	5.42	1.06
0.98	0.941	1.552	5	0.002194	0.00024	8.24	1.40
0.98	1.027	1.613	5	0.001174	0.00013	5.18	1.01
0.98	1.113	1.655	5	0.000866	0.00010	4.30	0.90
0.99	1.027	1.552	5	0.001721	0.00019	6.56	1.18
0.99	1.113	1.608	5	0.001058	0.00012	4.65	0.94
0.99	1.027	1.495	5	0.002671	0.00029	8.80	1.46
0.99	1.113	1.567	5	0.001306	0.00014	5.21	1.00
0.99	1.027	1.472	5	0.003176	0.00051	9.81	2.16
0.99	1.113	1.552	5	0.001346	0.00022	5.09	1.32

TABLE XIV: Bulk viscosity data determined from experimental sound attenuation measurements from the literature for xenon [16].

T/T_c	p/p_c	ρ/ρ_c	f/μs	α_λ	$\Delta\alpha_\lambda$	$\mu^*_{b,\mathrm{exp.}}$	$\Delta\mu^*_{b,\mathrm{exp.}}$
0.93	0.661	1.779	5	0.000717	0.00004	4.50	0.64
0.93	0.661	1.779	8	0.001073	0.00006	4.49	0.63
0.93	0.661	1.779	10	0.001596	0.00010	5.24	0.70
0.93	0.661	1.779	15	0.002068	0.00012	4.25	0.62
0.94	0.676	1.764	5	0.000819	0.00005	5.10	0.68
0.94	0.676	1.764	10	0.001638	0.00010	5.10	0.68
0.94	0.676	1.764	15	0.002242	0.00013	4.48	0.63
0.94	0.691	1.748	5	0.000840	0.00005	4.95	0.67

TABLE XIV: continued

T/T_c	p/p_c	ρ/ρ_c	f/μs	α_λ	$\Delta\alpha_\lambda$	$\mu^*_{b,\mathrm{exp.}}$	$\Delta\mu^*_{b,\mathrm{exp.}}$
0.94	0.691	1.748	10	0.001739	0.00010	5.19	0.69
0.94	0.691	1.748	15	0.002438	0.00015	4.73	0.65
0.94	0.706	1.731	5	0.001021	0.00006	6.02	0.75
0.94	0.706	1.731	10	0.001818	0.00011	5.16	0.68
0.94	0.706	1.731	15	0.002646	0.00016	4.95	0.66
0.95	0.721	1.714	10	0.002000	0.00012	5.47	0.70
0.95	0.721	1.714	15	0.002917	0.00018	5.27	0.68
0.95	0.737	1.697	5	0.001160	0.00007	6.19	0.76
0.95	0.737	1.697	7.5	0.001625	0.00010	5.66	0.71
0.95	0.737	1.697	10	0.002193	0.00013	5.75	0.72
0.95	0.737	1.697	15	0.003201	0.00019	5.55	0.70
0.95	0.752	1.679	5	0.001287	0.00008	6.57	0.78
0.95	0.752	1.679	10	0.002446	0.00010	6.15	0.59
0.95	0.752	1.679	15	0.003622	0.00014	6.05	0.58
0.96	0.785	1.640	5	0.001617	0.00010	7.48	0.85
0.96	0.785	1.640	7.5	0.002580	0.00010	8.06	0.70
0.96	0.785	1.640	10	0.003424	0.00014	8.02	0.70
0.96	0.785	1.640	15	0.004666	0.00019	7.12	0.64
0.96	0.793	1.629	5	0.001791	0.00011	8.13	0.90
0.96	0.802	1.619	10	0.003839	0.00015	8.47	0.73
0.97	0.819	1.597	10	0.004539	0.00018	9.48	0.78
0.97	0.836	1.573	5	0.002528	0.00015	9.80	1.03
0.97	0.836	1.573	7.5	0.003886	0.00023	10.09	1.05
0.97	0.836	1.573	10	0.005431	0.00022	10.65	0.85
0.97	0.836	1.573	15	0.007590	0.00030	9.81	0.80
0.97	0.853	1.548	5	0.003162	0.00019	11.50	1.17
0.97	0.853	1.548	7.5	0.004682	0.00028	11.33	1.15
0.97	0.853	1.548	10	0.006826	0.00027	12.55	0.97
0.97	0.853	1.548	15	0.009139	0.00037	11.02	0.87

TABLE XV: Results of the present relaxation ansatz Eq. (10)

T/T_c	p/p_c	ρ/ρ_c	c_f	δ_f	β_f	c_m	δ_m	β_m	c_s	δ_s	β_s	$\mu^*_{b,\mathrm{rel.}}$	$\Delta\mu^*_{b,\mathrm{rel.}}$
0.83	0.32	2.09	0.610	0.048	2.022	0.319	0.139	1.112	0.071	0.414	0.646	1.35	0.08
0.83	0.44	2.10	0.594	0.048	2.063	0.369	0.141	1.020	0.037	0.568	0.589	1.35	0.08
0.83	0.61	2.12	0.617	0.047	2.038	0.344	0.143	1.055	0.039	0.525	0.606	1.29	0.07
0.83	0.77	2.13	0.600	0.046	2.092	0.346	0.132	1.127	0.054	0.434	0.631	1.26	0.09
0.83	1.00	2.15	0.631	0.047	2.012	0.323	0.135	1.112	0.045	0.542	0.641	1.22	0.08
0.86	0.41	2.00	0.561	0.048	2.134	0.405	0.137	1.027	0.034	1.014	0.530	1.72	0.20
0.86	0.72	2.04	0.625	0.049	1.976	0.323	0.144	1.058	0.052	0.550	0.603	1.36	0.11
0.86	0.90	2.06	0.572	0.048	2.124	0.308	0.128	1.183	0.120	0.190	0.549	1.32	0.11
0.86	1.34	2.10	0.588	0.048	2.163	0.358	0.134	1.058	0.054	0.104	0.374	1.16	0.07
0.86	1.54	2.12	0.738	0.049	1.891	0.219	0.255	1.873	0.043	0.401	0.607	1.11	0.15
0.86	1.85	2.14	0.611	0.045	2.065	0.353	0.127	1.139	0.036	0.439	0.663	1.10	0.06
0.86	2.47	2.18	0.657	0.046	2.011	0.326	0.131	1.105	0.017	0.823	0.765	1.06	0.06
0.86	3.08	2.21	0.666	0.045	2.019	0.323	0.130	1.104	0.010	0.945	5.530	0.98	0.08
0.86	3.70	2.25	0.640	0.044	2.074	1.113	0.119	0.352	0.008	0.486	11.348	0.93	0.05
0.86	4.94	2.30	0.689	0.042	2.024	0.285	0.112	1.359	0.026	0.435	4.242	0.84	0.05
0.86	5.76	2.33	0.657	0.043	2.112	0.320	0.104	1.052	0.023	0.352	0.815	0.83	0.08
0.86	7.78	2.40	0.771	0.041	1.959	0.191	0.125	1.597	0.038	0.331	1.492	0.77	0.08
0.86	11.56	2.50	0.754	0.040	2.052	0.205	0.108	1.256	0.042	0.254	0.997	0.80	0.04
0.86	16.45	2.60	0.834	0.038	2.016	0.111	0.122	1.924	0.055	0.330	1.097	0.81	0.08
0.86	22.64	2.70	0.949	0.038	2.016	0.111	0.083	0.994	0.051	0.365	1.349	0.80	0.07
0.863	0.42	1.99	0.570	0.050	2.078	0.387	0.156	0.956	0.043	0.740	0.523	1.66	0.30

TABLE XV: continued

T/T_c	p/p_c	ρ/ρ_c	c_f	δ_f	β_f	c_m	δ_m	β_m	c_s	δ_s	β_s	$\mu^*_{b,\mathrm{rel.}}$	$\Delta\mu^*_{b,\mathrm{rel.}}$
0.863	2.47	2.17	0.634	0.045	2.031	0.301	0.118	1.246	0.066	0.315	0.793	1.03	0.06
0.863	3.08	2.21	0.647	0.046	2.060	0.346	0.124	1.053	0.006	0.944	0.611	0.98	0.09
0.863	4.94	2.30	0.694	0.043	2.004	0.291	0.125	1.190	0.015	0.511	1.263	0.85	0.08
0.863	7.93	2.40	0.843	0.043	1.942	0.100	0.149	3.540	0.057	0.332	1.340	0.85	0.08
0.863	11.73	2.50	0.769	0.041	2.044	0.218	0.117	1.226	0.013	0.585	1.659	0.75	0.05
0.863	16.64	2.60	0.839	0.039	2.027	0.100	0.127	1.548	0.061	0.284	1.012	0.77	0.13
0.863	22.85	2.70	0.835	0.038	2.058	0.159	0.135	0.870	0.006	1.481	0.877	0.83	0.09

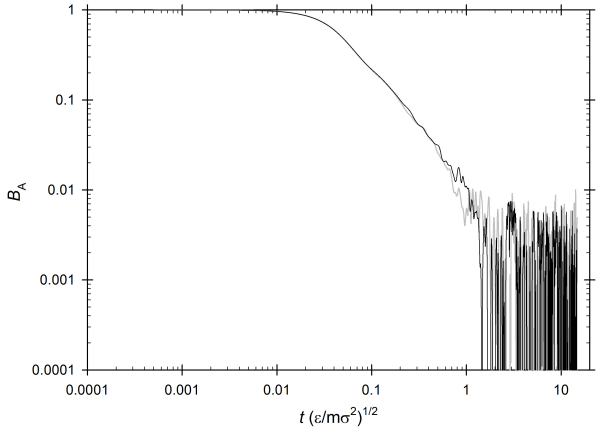

FIG. 4. Due to the similarity of both autocorrelation functions for simulations containing $N = 4096$ (grey) and $N = 12000$ particles (black), the results for the present relaxation ansatz are virtually identical.

[1] K. Singer and K. E. Gubbins, "Thermal transport coefficients for dense fluids," in *Statistical Mechanics. Volume 1*, edited by K. Singer (The Royal Society of Chemistry, 1973) pp. 194–253.
[2] R. Katti, R. T. Jacobsen, R. B. Stewart, and M. Jahangiri, "Thermodynamic Properties of Neon for Temperatures from the Triple Point to 700 K at Pressures to 700 MPa," in *Advances in Cryogenic Engineering*, edited by R. W. Fast (Springer, 1986) pp. 1189–1197.
[3] C. Tegeler, R. Span, and W. Wagner, J. Phys. Chem. Ref. Data **28**, 779 (1999).
[4] E. W. Lemmon and R. Span, J. Chem. Eng. Data **51**, 785 (2006).
[5] P. E. Mueller, D. Eden, C. W. Garland, and R. C. Williamson, Phys. Rev. A **6**, 2272 (1972).
[6] J. Thoen and C. W. Garland, Phys. Rev. A **10**, 1311 (1974).
[7] E. V. Larson, D. G. Naugle, and T. W. Aldair, J. Chem. Phys. **54**, 2429 (1971).
[8] P. Malbrunot, A. Boyer, E. Charles, and H. Abachi, Phys. Rev. A **27**, 1523 (1983).
[9] D. G. Naugle, J. H. Lunsford, and J. R. Singer, J. Chem. Phys. **45**, 4669 (1966).
[10] J. A. Cowan and R. N. Ball, Can. J. Phys. **50**, 1881 (1972).
[11] J. A. Cowan and P. W. Ward, Can. J. Phys. **51**, 2219 (1973).
[12] D. G. Naugle, J. Chem. Phys. **44**, 741 (1966).
[13] P. W. Ward, J. A. Cowan, and R. K. Pathria, Can. J. Phys. **53**, 29 (1975).
[14] J. A. Cowan and J. W. Leech, Can. J. Phys. **61**, 895 (1983).
[15] J. A. Cowan and R. N. Ball, Can. J. Phys. **58**, 74 (1980).
[16] J. A. Cowan and J. W. Leech, Can. J. Phys. **59**, 1280 (1981).